Atomic X-ray Spectrometry

X-ray spectroscopy, like optical spectroscopy, is based on measurement of emission, absorption, scattering, fluorescence, and diffraction of electromagnetic radiation. X-ray fluorescence and X-ray absorption methods are widely used for the qualitative and quantitative determination of all elements in the periodic table having atomic numbers greater than that of sodium. With special equipment, elements with atomic numbers in the range of 5 to 10 can also be determined.

Throughout this chapter, this logo indicates an opportunity for online self-study at **www.tinyurl.com/skoogpia7**, linking you to interactive tutorials, simulations, and exercises.

12A   FUNDAMENTAL PRINCIPLES

X-rays are short-wavelength electromagnetic radiation produced by the deceleration of high-energy electrons or by electronic transitions of electrons in the inner orbitals of atoms.[1] The wavelength range of X-rays is from about 10^{-5} Å to 100 Å; conventional X-ray spectroscopy is, however, largely confined to the region of about 0.1 Å to 25 Å (1 Å $= 0.1$ nm $= 10^{-10}$ m).

12A-1 Emission of X-rays

For analytical purposes, X-rays are generated in four ways: (1) by bombardment of a metal target with a beam of high-energy electrons, (2) by exposure of a substance to a primary beam of X-rays to generate a secondary beam of X-ray fluorescence (XRF), (3) by use of a radioactive source whose decay process results in X-ray emission,[2] and (4) from a synchrotron radiation source. Although small, compact synchrotron sources are under development, only about a dozen laboratories in the United States have facilities to produce X-rays from synchrotron radiation.[3] For this reason, we will consider only the first three sources.

X-ray sources, like ultraviolet and visible emitters, often produce both continuum and line spectra; both types are of importance in analysis. Continuum radiation is also called *white radiation* or *bremsstrahlung*. *Bremsstrahlung* means radiation

[1]For a more extensive discussion of the theory and analytical applications of X-rays, see M. Haschke, *Laboratory Micro-X-Ray Fluorescence Spectroscopy*, Heidelberg: Springer, 2014; B. E. Beckhoff, B. E. Kanngießer, N. E. Langhoff, R. E. Wedell, eds., *Handbook of Practical X-Ray Fluorescence Analysis*, New York: Springer, 2005; R. E. Van Grieken and A. A. Markowicz, eds., *Handbook of X-Ray Spectrometry*, 2nd ed., New York: Marcel Dekker, 2002; R. Jenkins, *X-Ray Fluorescence Spectrometry*, 2nd ed., New York: Wiley, 1999; R. Jenkins, R. W. Gould, and D. Gedcke, *Quantitative X-Ray Spectrometry*, 2nd ed., New York: Marcel Dekker, 1995.

[2]Electromagnetic radiation produced by radioactive sources is often called *gamma radiation*. Gamma radiation is indistinguishable from X-ray radiation.

[3]The high-intensity and collimated nature of beams from a synchrotron source leads to applications that cannot be accomplished by the other three X-ray sources. For a review of the applications of synchrotron-induced X-rays, see K. W. Jones and B. M. Gordon, *Anal. Chem.*, **1989**, *61*, 341A, **DOI**: 10.1021/ac00180a719; for a discussion of the use of total-reflectance XRF induced by synchrotron radiation, see R. Klockenkamper and A. von Bohlen, *Total Reflection X-Ray Fluorescence Analysis and Related Methods*, 2nd ed., Hoboken, NJ: Wiley, 2015; F. Meirer et al., *TrAC Trends Anal. Chem.*, **2010**, *29*, 479, **DOI**: 10.1016/j.trac.2010.04.001.

that arises from retardation of particles; such radiation is generally a spectral continuum.

Continuum Spectra from Electron Beam Sources

In an X-ray tube, electrons produced at a heated cathode are accelerated toward a metal anode (the *target*) by a potential difference as great as 100 kV. When electrons collide with the anode, part of the energy of the beam is converted to X-rays. Under some conditions, only a continuum spectrum such as that shown in Figure 12-1 results; under other conditions, a line spectrum is superimposed on the continuum (see Figure 12-2).

The continuum X-ray spectrum shown in the two figures is characterized by a well-defined, short-wavelength limit (λ_0), which depends on the accelerating voltage V but is independent of the target material. Thus, λ_0 (0.35 Å) for the spectrum produced with a molybdenum target at 35 kV (Figure 12-2) is identical to λ_0 for a tungsten target at the same voltage (Figure 12-1).

The continuum radiation from an electron beam source results from collisions between the electrons of the beam and the atoms of the target material. At each collision, the electron is decelerated and a photon of X-ray energy is produced. The energy of the photon is equal to the difference in kinetic energies of the electron before and after the collision. Generally, the electrons in a beam are decelerated in a series of collisions; the resulting loss of kinetic energy differs from collision to collision. Thus, the energies of the emitted X-ray photons vary continuously over a considerable range. The maximum photon energy generated corresponds to the instantaneous deceleration of the electron to zero kinetic energy in a single collision. For such an event, we can write

$$h\nu_0 = \frac{hc}{\lambda_0} = Ve \tag{12-1}$$
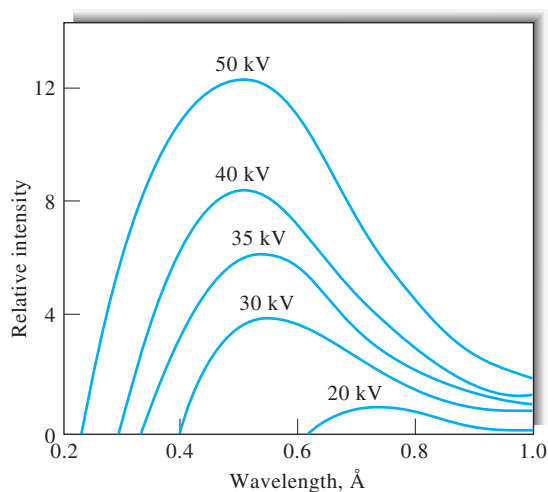
FIGURE 12-1 Distribution of continuum radiation from an X-ray tube with a tungsten target. The numbers above the curves indicate the accelerating voltages.
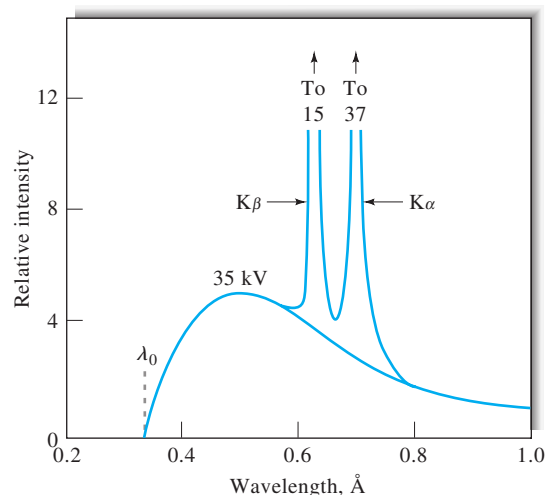
FIGURE 12-2 Line spectrum for an X-ray with a molybdenum target.

where Ve, the product of the accelerating voltage and the charge on the electron, is the kinetic energy of all of the electrons in the beam; h is Planck's constant; and c is the velocity of light. The quantity ν_0 is the maximum frequency of radiation that can be produced at voltage V, and λ_0 is the low wavelength limit for the radiation. This relationship is known as the *Duane-Hunt law*. It is interesting to note that Equation 12-1 provides a direct means for the highly accurate determination of Planck's constant. When we substitute numerical values for the constants and rearrange, Equation 12-1 becomes

$$\lambda_0 = 12{,}398/V \tag{12-2}$$

where λ_0 and V have units of angstroms and volts, respectively.

Line Spectra from Electron Beam Sources

As shown in Figure 12-2, bombardment of a molybdenum target produces intense emission lines at about 0.63 and 0.71 Å; an additional simple series of lines occurs in the longer-wavelength range of 4 to 6 Å.

The emission behavior of molybdenum is typical of all elements having atomic numbers larger than 23; that is, the X-ray line spectra are remarkably simple when compared with ultraviolet emission and consist of two series of lines. The shorter-wavelength group is called the K series and the other the L series.[4] Elements with atomic numbers smaller than 23 produce only a K series. Table 12-1 presents wavelength data for the emission spectra of a few elements.

A second characteristic of X-ray spectra is that the minimum acceleration voltage required for the excitation of the

---

[4]For the heavier elements, additional series of lines (M, N, and so forth) are found at longer wavelengths. Their intensities are low, however, and little use is made of them. The designations K and L arise from the German words *kurtz* and *lang* for short and long wavelengths. The additional alphabetical designations were then added for lines occurring at progressively longer wavelengths.
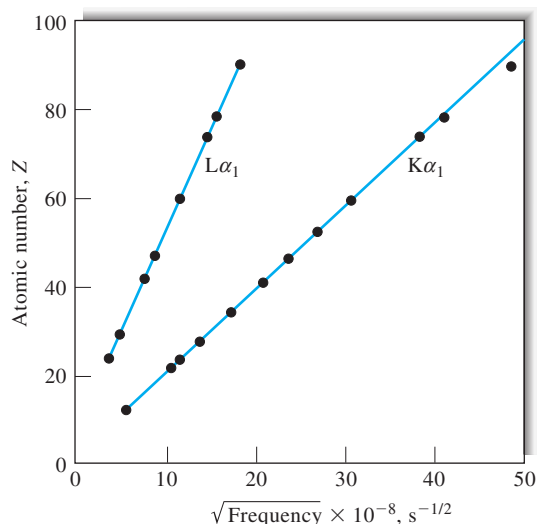
TABLE 12-1 Wavelengths in Angstroms of the More Intense Emission Lines for Some Typical Elements

Element	Atomic Number	K Series		L Series	
		α_1	β_1	α_1	β_1
Na	11	11.909	11.617	—	—
K	19	3.742	3.454	—	—
Cr	24	2.290	2.085	21.714	21.323
Rb	37	0.926	0.829	7.318	7.075
Cs	55	0.401	0.355	2.892	2.683
W	74	0.209	0.184	1.476	1.282
U	92	0.126	0.111	0.911	0.720

FIGURE 12-3 Relationship between X-ray emission frequency and atomic number for $K\alpha_1$ and $L\alpha_1$ lines.

lines for each element increases with atomic number. Thus, the line spectrum for molybdenum (atomic number = 42) disappears if the excitation voltage drops below 20 kV. As shown in Figure 12-1, bombardment of tungsten (atomic number = 74) produces no lines in the region of 0.1 to 1.0 Å, even at 50 kV. Characteristic K lines appear at 0.18 and 0.21 Å, however, if the voltage increases to 70 kV.

Figure 12-3 illustrates the linear relationship between the square root of the frequency for a given (K or L) line and the atomic number of the element responsible for the radiation. This property was first discovered by English physicist H. G. J. Moseley in 1914.[5]

X-ray line spectra result from electronic transitions that involve the innermost atomic orbitals. The short-wavelength K series is produced when the high-energy electrons from the cathode remove electrons from those orbitals nearest the nucleus of the target atom. The collision results in the formation of excited *ions*, which then emit quanta of X-radiation as electrons from outer orbitals undergo transitions to the vacant orbital. As shown in Figure 12-4, the lines in the K series arise from electronic transitions between higher energy levels and the K shell. The L series of lines result when an electron is lost from the second principal quantum level, either as a result of ejection by an electron from the cathode or from the transition

of an L electron to the K level that accompanies the production of a quantum of K radiation. It is important to appreciate that the energy scale in Figure 12-4 is logarithmic. Thus, the energy difference between the L and K levels is significantly larger than that between the M and L levels. The K lines therefore appear at shorter wavelengths. It is also important to note that the energy differences between the transitions labeled α_1 and α_2 as well as those between β_1 and β_2 are so small that only single lines are observed in all but the highest-resolution spectrometers (see Figure 12-2).

The energy level diagram in Figure 12-4 is applicable to any element with sufficient electrons to permit the number of transitions shown. The differences in energies between the levels increase regularly with atomic number because of the increasing charge on the nucleus; therefore, the radiation for the K series appears at shorter wavelengths for the heavier elements (see Table 12-1). The effect of nuclear charge is also reflected in the increase in minimum voltage required to excite the spectra of these elements.

It is important to note that for all but the lightest elements, the wavelengths of characteristic X-ray lines are independent of the physical and chemical state of the element because the transitions responsible for these lines involve electrons that take no part in bonding. Thus, the position of the $K\alpha$ lines for molybdenum is the same regardless of whether the target is the pure metal, its sulfide, or its oxide.

Line Spectra from Fluorescent Sources

Another convenient way of producing a line spectrum is to irradiate the element or one of its compounds with the continuum radiation from an X-ray tube. This process is explored further in a later section.

---

[5]Henry Gwyn Jeffreys Moseley (1887–1915) discovered this important relationship, which is now called Moseley's law, while working with Ernest Rutherford at the University of Manchester. His studies revealed gaps in the sequence of atomic numbers at 43, 61, 72, 75, and 87, which are now filled by the elements technetium, promethium, hafnium, rhenium, and francium—all subsequently discovered or produced artificially. When World War I broke out, Moseley enlisted in the Royal Engineers and was killed by a sniper while serving in Gallipoli. It is thought that his tragic death was the driving force to forbid British scientists from serving in combat. If he had lived, Moseley would likely have received the Nobel Prize for his groundbreaking research. For more details on Moseley's life and work, see R. Porter and M. Ogilvie, eds., *The Biographical Dictionary of Scientists*, 3rd ed., New York: Oxford, 2000.
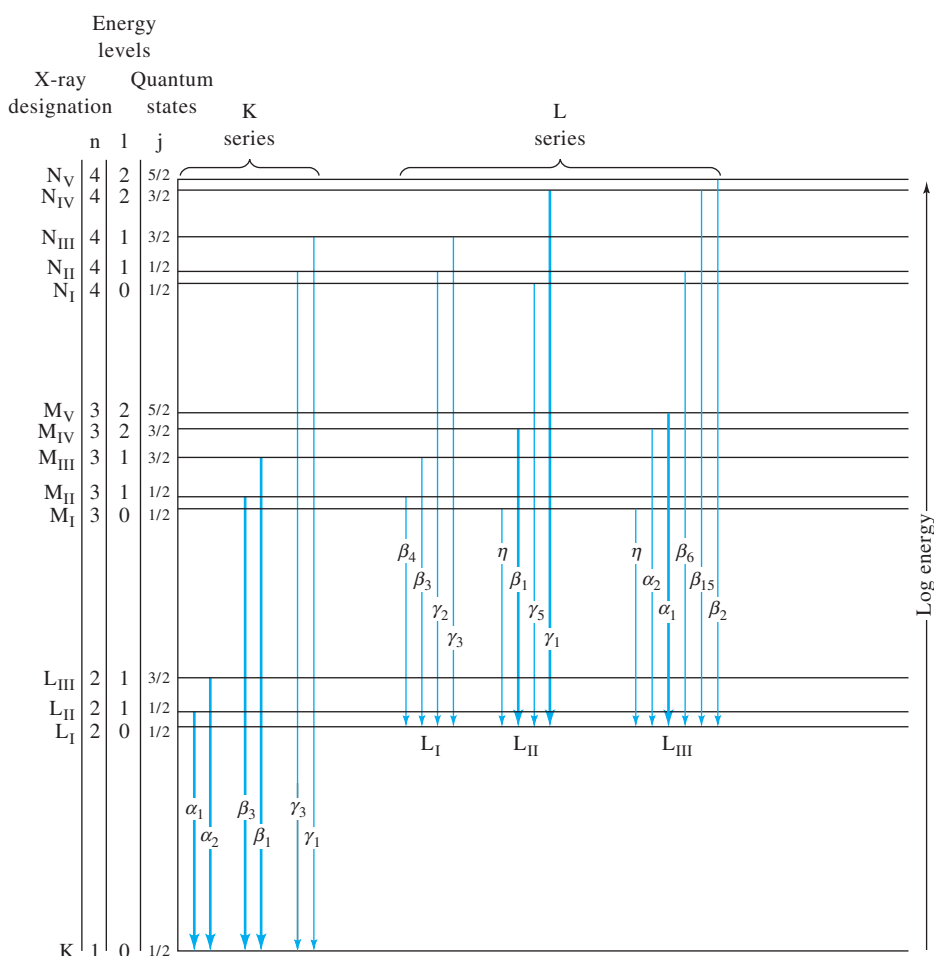
FIGURE 12-4 Partial energy level diagram showing common transitions producing X-rays. The most intense lines are indicated by the wider arrows.

Spectra from Radioactive Sources

X-radiation is often a product of radioactive decay processes. *Gamma rays*, which are indistinguishable from X-rays, are produced in intranuclear reactions. Many α and β emission processes (see Section 32A-2) leave a nucleus in an excited state; the nucleus then releases one or more quanta of gamma rays as it returns to its ground state. *Electron capture* or *K capture* also produces X-radiation. This process involves capture of a K electron (less commonly, an L or an M electron) by the nucleus and formation of an element of the next lower atomic number. As a result of K capture, electronic transitions to the vacated orbital occur, and we observe the X-ray line spectrum of the newly formed element. The half-lives of K-capture processes range from a few minutes to several thousand years.

Artificially produced radioactive isotopes provide a very simple source of monoenergetic radiation for certain analytical applications. The best-known example is iron-55, which undergoes a K-capture reaction with a half-life of 2.6 years:

$$^{55}_{26}\text{Fe} \rightarrow \, ^{55}_{25}\text{Mn} + h\nu$$
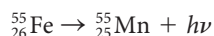
The resulting manganese Kα line at about 2.1 Å has proved to be a useful source for both fluorescence and absorption methods. Table 12-2 lists some additional common radioisotopic sources for X-ray spectroscopy.

12A-2 Absorption Spectra

When a beam of X-rays is passed through a thin layer of matter, its intensity, or power, is generally diminished as a result of absorption and scattering. The effect of scattering for all but the lightest elements is ordinarily small and can be neglected in those wavelength regions where appreciable absorption occurs. As shown in Figure 12-5, the absorption spectrum of an element, like its emission spectrum, is simple and consists of a few well-defined absorption peaks. Here again, the wavelengths of the absorption maxima are characteristic of the element and are largely independent of its chemical state.

A peculiarity of X-ray absorption spectra is the appearance of sharp discontinuities, called *absorption edges*, at wavelengths immediately beyond absorption maxima.

TABLE 12-2 Common Radioisotopic Sources for X-ray Spectroscopy

| Source	Decay Process	Half-Life	Type of Radiation	Energy, keV
$^{3}_{1}$H-Ti[a]	β^-	12.3 years	Continuum	3–10
			Ti-K X-rays	4–5
$^{55}_{26}$Fe	EC[b]	2.7 years	Mn-K X-rays	5.9
$^{57}_{27}$Co	EC	270 days	Fe-K X-rays	6.4
			γ rays	14, 122, 136
$^{109}_{48}$Cd	EC	1.3 years	Ag-K X-rays	22
			γ rays	88
$^{125}_{53}$I	EC	60 days	Te-K X-rays	27
			γ rays	35
$^{147}_{61}$Pm-Al	β^-	2.6 years	Continuum	12–45
$^{210}_{82}$Pb	β^-	22 years	Bi-L X-rays	11
			γ rays	47

[a]Tritium adsorbed on nonradioactive titanium metal.

[b]EC = Electron capture.

The Absorption Process

Absorption of an X-ray quantum causes ejection of one of the innermost electrons from an atom, which results in the production of an excited ion. In this process, the entire energy $h\nu$ of the radiation is partitioned between the kinetic energy of the electron (the *photoelectron*) and the potential energy of the excited ion. The highest probability for absorption occurs when the energy of the quantum is exactly equal to the energy required to remove the electron just to the periphery of the atom (that is, as the kinetic energy of the ejected electron approaches zero).

The absorption spectrum for lead, shown in Figure 12-5, exhibits four peaks, the first occurring at 0.14 Å. The energy of the quantum corresponding to this wavelength exactly matches the energy required to just eject the highest-energy K electron of the element. At wavelengths just larger than this wavelength, the energy of the radiation is insufficient to bring about removal of a K electron, and an abrupt decrease in absorption occurs. At
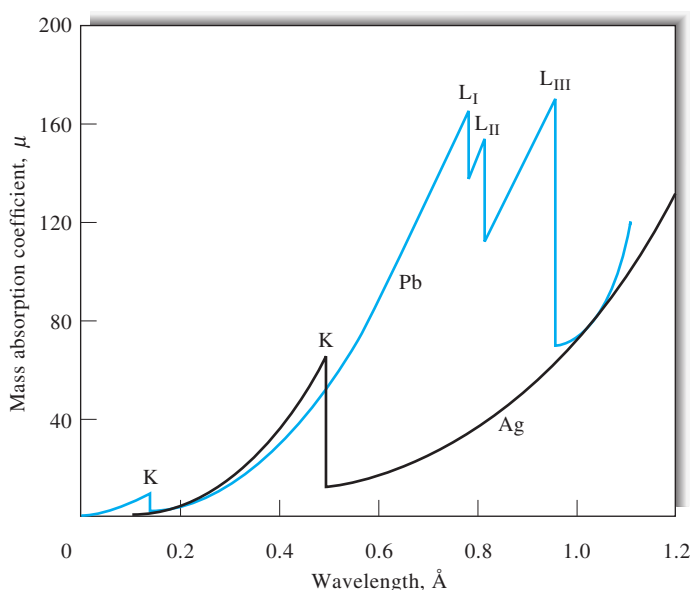
FIGURE 12-5 X-ray absorption spectra for lead and silver.

wavelengths shorter than 0.14 Å, the probability of interaction between the electron and the radiation gradually diminishes; this results in a smooth decrease in absorption. In this region, the kinetic energy of the ejected photoelectron increases continuously with the decrease in wavelength.

The additional peaks at longer wavelengths correspond to the removal of an electron from the L energy levels of lead. Three sets of L levels, differing slightly in energy, exist (see Figure 12-4); three maxima are, therefore, observed. Another set of lines, arising from ejections of M electrons, are located at longer wavelengths, which are not shown in Figure 12-5.

Figure 12-5 also shows the K absorption edge for silver, which occurs at 0.485 Å. The longer wavelength for silver reflects its lower atomic number than that of lead.

The Mass Absorption Coefficient

Beer's law applies to the absorption of X-radiation, so we may write

$$\ln\frac{P_0}{P} = \mu x$$

where x is the sample thickness in centimeters and P and P_0 are the powers of the transmitted and incident beams, respectively. The constant μ is called the *linear absorption coefficient* and is characteristic of the element as well as the number of its atoms in the path of the beam. A more convenient form of Beer's law is

$$\ln\frac{P_0}{P} = \mu_M \rho x \qquad (12\text{-}3)$$

where ρ is the density of the sample and μ_M is the *mass absorption coefficient*, a quantity that is *independent* of the physical and chemical state of the element. Thus, the mass absorption coefficient for bromine has the same value in gaseous HBr as in solid sodium bromate. Note that the mass absorption coefficient carries units of cm^2/g.

Mass absorption coefficients are additive functions of the weight fractions of elements contained in a sample. Thus,

$$\mu_M = W_A\mu_A + W_B\mu_B + W_C\mu_C + \cdots \qquad (12\text{-}4)$$

where μ_M is the mass absorption coefficient of a sample containing the weight fractions W_A, W_B, and W_C of elements A, B, and C. The terms μ_A, μ_B, and μ_C are the respective mass absorption coefficients for each of the elements. Tables of mass absorption coefficients for the elements at various wavelengths are found in many handbooks, monographs, and research papers and on the web.[6]

Tutorial: Learn more about **X-ray absorption and fluorescence** at www.tinyurl.com/skoogpia7

[6]For example, J. H. Hubbell, *International Journal of Applied Radiation and Isotopes*, **1982**, *33*, 1269, **DOI**: 10.1016/0020-708X(82)90248-4 and http://physics .nist.gov/PhysRefData/XrayMassCoef/cover.html.

12A-3 X-ray Fluorescence

The absorption of X-rays produces electronically excited ions that return to their ground state by transitions involving electrons from higher energy levels. Thus, an excited ion with a vacant K shell is produced when lead absorbs radiation of wavelengths shorter than 0.14 Å (Figure 12-5); after a brief period, the ion returns to its ground state via a series of electronic transitions characterized by the emission of X-radiation (fluorescence) of wavelengths identical to those that result from excitation produced by electron bombardment. The wavelengths of the fluorescence lines are always somewhat greater than the wavelength of the corresponding absorption edge, however, because absorption requires a complete removal of the electron (that is, ionization), whereas emission involves transitions of an electron from a higher energy level within the ion. For example, the K absorption edge for silver occurs at 0.485 Å, but the K emission lines for the element have wavelengths at 0.497 and 0.559 Å. When fluorescence is to be excited by radiation from an X-ray tube, the operating voltage must be sufficiently great so that the cutoff wavelength λ_0 (Equation 12-2) is shorter than the absorption edge of the element whose spectrum is to be excited. Thus, to generate the K lines for silver, the tube voltage would need to be (Equation 12-2)

$$V \geq \frac{12,398 \text{ V} \cdot \text{Å}}{0.485 \text{ Å}} = 25,560 \text{ V or } 25.6 \text{ kV}$$

Analytical methods using XRF are described in Section 12C.

12A-4 Diffraction of X-rays

Like other types of electromagnetic radiation, when X-radiation passes through a sample of matter, the electric vector of the radiation interacts with the electrons in the atoms of the matter to produce scattering. When X-rays are scattered by the ordered environment in a crystal, constructive and destructive interference occurs among the scattered rays because the distances between the scattering centers are of the same order of magnitude as the wavelength of the radiation. Diffraction is the result.

Bragg's Law

When an X-ray beam strikes a crystal surface at some angle θ, part of the beam is scattered by the layer of atoms at the surface. The unscattered part of the beam penetrates to the second layer of atoms where again a fraction is scattered, and the remainder passes on to the third layer (Figure 12-6), and so on. The cumulative effect of this scattering from the regularly spaced centers of the crystal is diffraction of the beam in much the same way as visible radiation is diffracted by a reflection grating (Section 7C-2). The requirements for X-ray diffraction are (1) the spacing between layers of atoms must be roughly the same as the wavelength of the radiation and (2) the scattering centers must be spatially distributed in a highly regular way.

Simulation: Learn more about **X-ray diffraction** at www.tinyurl.com/skoogpia7
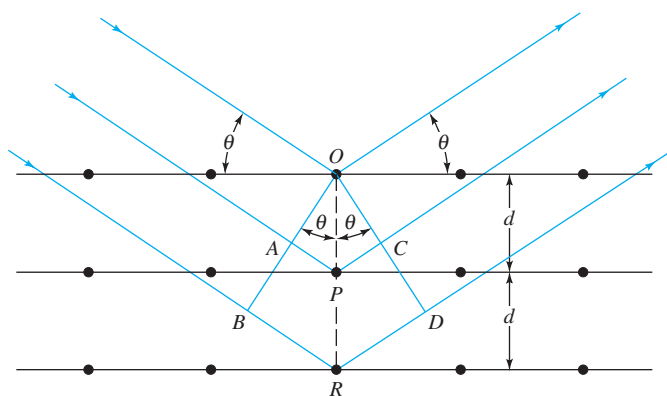
FIGURE 12-6 Diffraction of X-rays by a crystal.

In 1912, W. L. Bragg treated the diffraction of X-rays by crystals as shown in Figure 12-6. Here, a narrow beam of radiation strikes the crystal surface at angle θ; scattering occurs as a result of interaction of the radiation with atoms located at O, P, and R. If the distance

$$AP + PC = \mathbf{n}\lambda$$

where $\mathbf{n}$ is an integer, the scattered radiation will be in phase at OCD, and the crystal will appear to reflect the X-radiation. But

$$AP = PC = d \sin \theta \qquad (12\text{-}5)$$

where d is the interplanar distance of the crystal. Thus, the conditions for constructive interference of the beam at angle θ are

$$\mathbf{n}\lambda = 2d \sin \theta \qquad (12\text{-}6)$$

Equation 12-6 is the fundamentally important *Bragg equation*. Note that X-rays appear to be reflected from the crystal only if the angle of incidence satisfies the condition

$$\sin \theta = \frac{\mathbf{n}\lambda}{2d}$$

At all other angles, destructive interference occurs.

12B INSTRUMENT COMPONENTS

Absorption, emission, fluorescence, and diffraction of X-rays are all applied in analytical chemistry. Instruments for these applications contain components that are analogous in function to the five components of instruments for optical spectroscopic measurement; these components include a source, a device for restricting the wavelength range of incident radiation, a sample holder, a radiation detector or transducer, and a signal processor and readout. These components differ considerably in detail from the corresponding optical components. Their functions, however, are the same, and the ways they combine to form instruments are often similar to those shown in Figure 7-1.

As with optical instruments, both X-ray photometers and spectrophotometers are encountered, the first using filters and the second using monochromators to transmit radiation of the desired wavelength from the source. In addition, however, a third method is available for obtaining information about isolated portions of an X-ray spectrum. Here, isolation is achieved electronically with devices that discriminate among various parts of a spectrum based on the *energy* rather than the *wavelength* of the radiation. Thus, X-ray instruments are often described as *wavelength-dispersive instruments* or *energy-dispersive instruments*, depending on the method by which they resolve spectra.

12B-1 Sources

Three types of sources are used in X-ray instruments: tubes, radioisotopes, and secondary fluorescence sources.

The X-ray Tube

The most common source of X-rays for analytical work is the X-ray tube (sometimes called a *Coolidge tube*), which can take a variety of shapes and forms; one design is shown schematically in Figure 12-7. An X-ray source is a highly evacuated tube in which is mounted a tungsten filament cathode and a massive anode. The anode generally consists of a heavy block of copper with a metal target plated on or embedded in the surface of the copper. Target materials include such metals as tungsten, chromium, copper, molybdenum, rhodium, scandium, silver, iron, and cobalt. Separate circuits are used to heat the filament and to accelerate the electrons to the target. The heater circuit provides the means for controlling the intensity of the emitted X-rays, whereas the accelerating voltage determines their energy, or wavelength. For quantitative work, both circuits must be operated with stabilized power supplies that control the current or the voltage to 0.1% relative.

The production of X-rays by electron bombardment is a highly inefficient process. Less than 1% of the electrical power is converted to radiant power, the remainder being dissipated
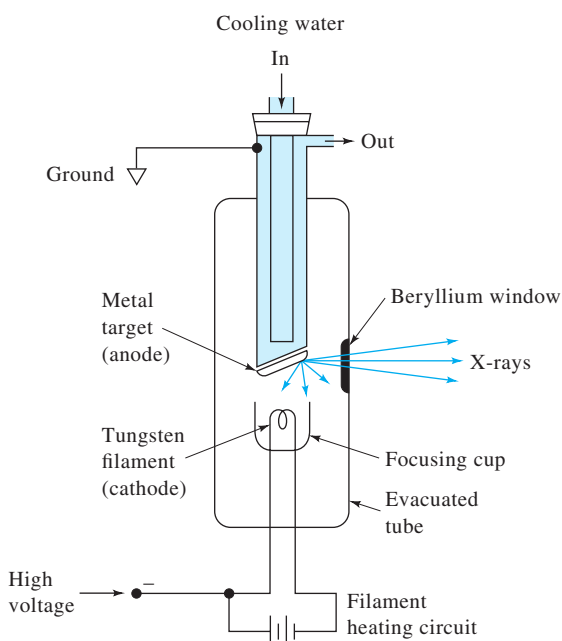
Cooling water

FIGURE 12-7 Schematic of an X-ray tube.

as heat. As a result, until relatively recently, water cooling of the anodes of X-ray tubes was required. With modern equipment, however, cooling is often unnecessary because tubes can be operated at less than 50 W of power, substantially lower than the 1 kW or more of high-power tubes. This reduction in power is made possible by the greater sensitivity of modern X-ray transducers.

Radioisotopes

A variety of radioactive substances have been used as sources in XRF and absorption methods (see Table 12-2). Generally, the radioisotope is encapsulated to prevent contamination of the laboratory and shielded to absorb radiation in all but certain directions.

Many of the best radioactive sources provide simple line spectra; others produce a continuum (see Table 12-2). Because of the shape of X-ray absorption curves, a given radioisotope will be suitable for excitation of fluorescence or for absorption studies for a range of elements. For example, a source producing a line in the region between 0.30 and 0.47 Å is suitable for fluorescence or absorption studies involving the K absorption edge for silver (see Figure 12-5). Sensitivity improves as the wavelength of the source line approaches the absorption edge. Iodine-125 with a line at 0.46 Å is ideal for determining silver from this standpoint.

Secondary Fluorescent Sources

In some applications, the fluorescence spectrum of an element that has been excited by radiation from an X-ray tube serves as a source for absorption or fluorescence studies. This arrangement has the advantage of eliminating the continuum emitted by the

primary source. For example, an X-ray tube with a tungsten target (Figure 12-1) could be used to excite the Kα and Kβ lines of molybdenum (Figure 12-2). The resulting fluorescence spectrum would then be similar to the spectrum in Figure 12-2 except that the continuum would be absent.

12B-2 Filters for X-rays

In many applications, it is desirable to use an X-ray beam with a narrow wavelength range. As in the visible region, both filters and monochromators are used for this purpose.

Figure 12-8 illustrates a common technique for producing a relatively monochromatic beam by use of a filter. Here, the Kβ line and most of the continuum emitted from a molybdenum target is removed by a zirconium filter having a thickness of about 0.01 cm. The pure Kα line is then available for analytical purposes. Several other target-filter combinations of this type have been developed, each of which serves to isolate one of the intense lines of a target element. Monochromatic radiation produced in this way is widely used in X-ray diffraction studies. The choice of wavelengths available by this technique is limited by the relatively small number of target-filter combinations that are available.

Filtering the continuum from an X-ray tube is also feasible with thin strips of metal. As with glass filters for visible radiation, relatively broad bands are transmitted with a significant attenuation of the desired wavelengths.

12B-3 X-ray Monochromators

Figure 12-9 shows the essential components of an X-ray spectrometer. The monochromator consists of a pair of beam collimators, which serve the same purpose as the slits in an
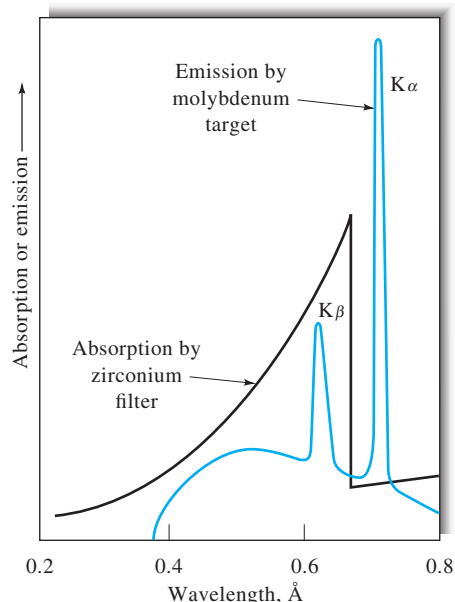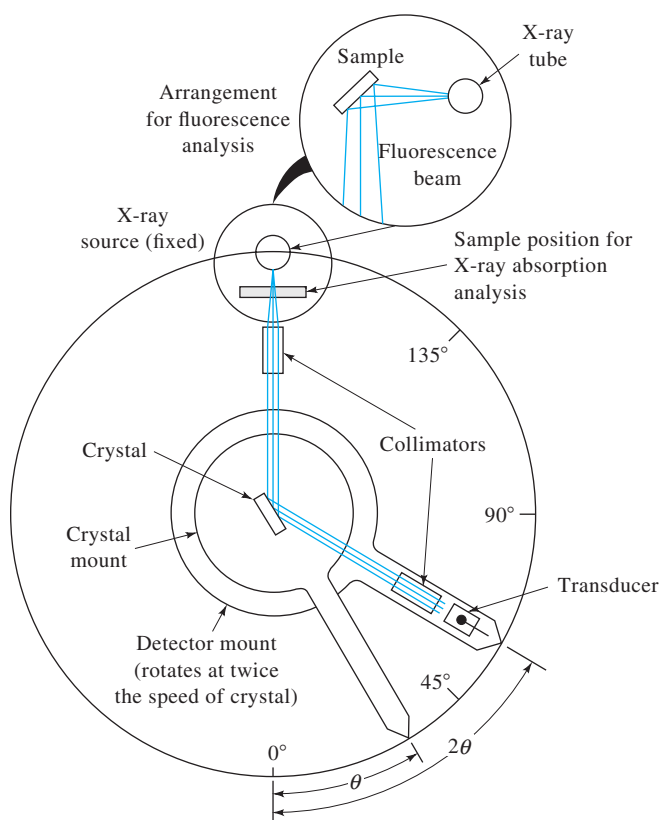

FIGURE 12-8 Use of a filter to produce monochromatic radiation.

FIGURE 12-9 An X-ray monochromator and detector. Note that the angle of the detector with respect to the beam (2θ) is twice that of the crystal face. For absorption analysis, the source is an X-ray tube and the sample is located in the beam as shown. For emission measurements, the sample becomes a source of XRF as shown in the insert.

optical instrument, and a dispersing element. The latter is a single crystal mounted on a *goniometer*, or rotatable table, that permits variation and precise determination of the angle θ between the crystal face and the collimated incident beam. From Equation 12-6, it is evident that, for any given angular setting of the goniometer, only a few wavelengths are diffracted $(\lambda, \lambda/2, \lambda/3, \ldots, \lambda/\mathbf{n}$, where $\lambda = 2d \sin \theta)$.

To produce a spectrum, it is necessary that the exit beam collimator and the detector be mounted on a second table that rotates at twice the rate of the first; that is, as the crystal rotates through an angle θ, the detector must simultaneously move through an angle 2θ. Clearly, the interplanar spacing *d* for the crystal must be known precisely (Equation 12-6). Many modern X-ray monochromators have computer-controlled motors to drive the crystal and the detector independently without a gear-based mechanical connection. These units are capable of scanning at very rapid rates (ca. 240°/min). Some instruments feature slew-scan operation, in which the monochromator can be slewed to the wavelength region of interest (ca. 1400°/min) and then slowly scanned over analyte peaks.

The collimators for X-ray monochromators ordinarily consist of a series of closely spaced metal plates or tubes that absorb all but the parallel beams of radiation.

X-radiation longer than about 2 Å is absorbed by constituents of the atmosphere. Therefore, provision is usually made for a continuous flow of helium through the sample compartment and monochromator when longer wavelengths are required. Alternatively, these areas can be evacuated by pumping.

The loss of intensity is high in a monochromator equipped with a flat crystal because as much as 99% of the radiation is sufficiently divergent to be absorbed in the collimators. Increased intensities, by as much as a factor of 10, have been achieved by using a curved crystal surface that acts not only to diffract but also to focus the divergent beam from the source on the exit collimator.

As illustrated in Table 12-1, most analytically important X-ray lines lie in the region between about 0.1 and 10 Å. The data in Table 12-3, however, lead to the conclusion that no single crystal satisfactorily disperses radiation over this entire range. As a result, an X-ray monochromator must be provided with at least two (and preferably more) interchangeable crystals.

The useful wavelength range for a crystal is determined by its lattice spacing *d* and the problems associated with detection of the radiation when 2θ approaches zero or 180°. When a monochromator is set at angles of 2θ that are much less than 10°, the amount of polychromatic radiation scattered from the crystal surface becomes prohibitively high. Generally, values of 2θ greater than about 160° cannot be measured because the location of the source unit prohibits positioning of the detector at such an angle (see Figure 12-9). The minimum and maximum values for λ in Table 12-3 were determined from these limitations.

Table 12-3 shows that a crystal with a large lattice spacing, such as ammonium dihydrogen phosphate ($NH_4H_2PO_4$), has a much greater wavelength range than a crystal in which this variable is small. The advantage of large values of *d* is offset, however, by the resulting lower dispersion. This effect can be seen by differentiation of Equation 12-6, which leads to

$$\frac{d\theta}{d\lambda} = \frac{\mathbf{n}}{2d \cos \theta}$$

Here, $d\theta/d\lambda$, a measure of dispersion, is seen to be inversely proportional to *d*. Table 12-3 provides dispersion data for the various crystals at their maximum and minimum wavelengths. The low dispersion of $NH_4H_2PO_4$ prohibits its use in the region of short wavelengths; here, a crystal such as topaz or lithium fluoride must be substituted.

12B-4 X-ray Transducers and Signal Processors

Early X-ray equipment used photographic emulsions for detection and recording of radiation. For convenience, speed, and accuracy, however, modern instruments are generally equipped with transducers that convert radiant energy into an

TABLE 12-3 Properties of Typical Diffracting Crystals

| Crystal | Lattice Spacing d, Å | Wavelength Range,[a] Å | | Dispersion, °/Å | |
		λ_{max}	λ_{min}	at λ_{max}	at λ_{min}
Topaz	1.356	2.67	0.24	2.12	0.37
LiF	2.014	3.97	0.35	1.43	0.25
NaCl	2.820	5.55	0.49	1.02	0.18
EDDT[b]	4.404	8.67	0.77	0.65	0.11
ADP[c]	5.325	10.50	0.93	0.54	0.09

[a]Based on the assumption that the measurable range of 2θ is from 160° for λ_{max} to 10° for λ_{min}.

[b]EDDT = Ethylenediamine d-tartrate.

[c]ADP = Ammonium dihydrogen phosphate.

electrical signal. Three types of transducers are used: *gas-filled transducers*, *scintillation counters*, and *semiconductor transducers*. Before considering the function of each of these devices, it is worthwhile to discuss *photon counting*, a signal-processing method that is often used with X-ray transducers as well as detectors of radiation from radioactive sources (Chapter 32) and some ultraviolet-visible sources (Section 7F-1).

Photon Counting

In contrast to the various photoelectric detectors we have thus far considered, X-ray detectors are usually operated as *photon counters*. In this mode of operation, individual pulses of charge are produced as quanta of radiation, are absorbed by the transducer, and are counted; the power of the beam is then recorded digitally as the number of counts per unit of time. Photon counting requires rapid response times for the transducer and signal processor so that the arrival of individual photons may be accurately detected and recorded. In addition, the technique is applicable only to beams of relatively low intensity. As the beam intensity increases, photon pulses begin to overlap and only a steady-state current, which represents an average number of pulses per second, can be measured. If the response time of the transducer is long, pulse overlap occurs at relatively low photon intensities. As its response time becomes shorter, the transducer is more capable of detecting individual photons without pulse overlap.[7]

For weak sources of radiation, photon counting generally provides more accurate intensity data than are obtainable by measuring average currents. The improvement can be traced to

Exercise: Learn more about **X-ray spectrometers** at www.tinyurl.com/skoogpia7

[7]E. J. Darland, G. E. Leroi, and C. G. Enke, *Anal. Chem.*, **1980**, *52*, 714, **DOI**: 10.1021/ac50054a028.

signal pulses being generally substantially larger than the pulses arising from background noise in the source, transducer, and associated electronics; separation of the signal from noise can then be achieved with a *pulse-height discriminator*, an electronic device that is discussed further in Section 12B-5.

Photon counting is used in X-ray work because the power of available sources is often low. In addition, photon counting permits spectra to be acquired without using a monochromator. This property is considered in the section devoted to energy-dispersive systems.

Gas-Filled Transducers

When X-radiation passes through an inert gas such as argon, xenon, or krypton, interactions occur that produce a large number of positive gaseous ions and electrons (ion pairs) for each X-ray quantum. Three types of X-ray transducers, *ionization chambers*, *proportional counters*, and *Geiger tubes*, are based on the enhanced conductivity of the gas resulting from this phenomenon.

A typical gas-filled transducer is shown schematically in Figure 12-10. Radiation enters the chamber through a transparent window of mica, beryllium, aluminum, or Mylar. Each photon of X-radiation that interacts with an atom of argon causes it to lose one of its outer electrons. This *photoelectron* has a large kinetic energy, which is equal to the difference between the X-ray photon energy and the binding energy of the electron in the argon atom. The photoelectron then loses this excess kinetic energy by ionizing several hundred additional atoms of the gas. Under the influence of an applied voltage, the mobile electrons migrate toward the central wire anode and the slower-moving cations migrate toward the cylindrical metal cathode.

Figure 12-11 shows the effect of applied voltage on the number of electrons that reach the anode of a gas-filled transducer for each entering X-ray photon. The diagram indicates three characteristic voltage regions. At voltages less than V_1, the accelerating force on the ion pairs is low, and the rate the positive and negative species separate is insufficient to prevent partial recombination. As a result, the number of electrons reaching the anode is smaller than the number produced initially by the incoming radiation.
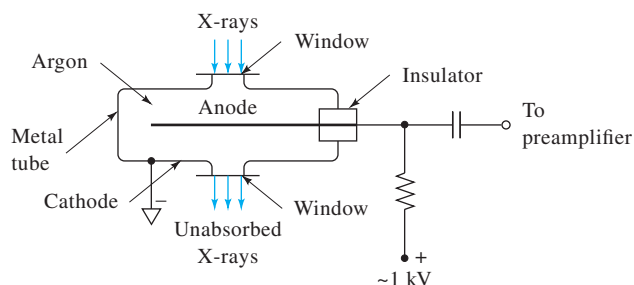
FIGURE 12-10 Cross section of a gas-filled detector.
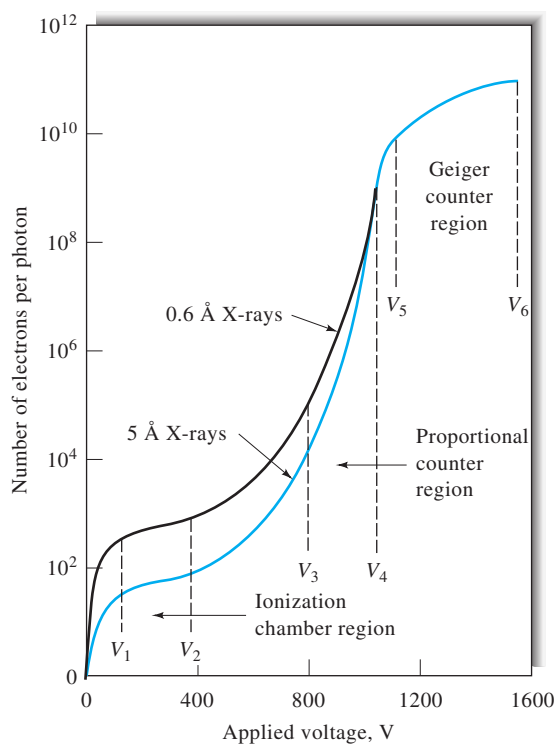
FIGURE 12-11 Gas amplification for various types of gas-filled detectors.

In the *ionization chamber region* between V_1 and V_2, the number of electrons reaching the anode is reasonably constant and represents the total number formed by a single photon.

In the *proportional counter region* between V_3 and V_4, the number of electrons increases rapidly with applied voltage. This increase is the result of secondary ion-pair production caused by collisions between the accelerated electrons and gas molecules. In the proportional counter region, amplification of the ion current (*gas amplification*) occurs.

In the *Geiger range* V_5 to V_6, amplification of the electrical pulse is enormous but is limited by the positive space charge created as the faster-moving electrons migrate away from the slower positive ions. Because of this effect, the number of electrons reaching the anode is independent of the type and energy of incoming radiation and is governed instead by the geometry and gas pressure of the tube.

Figure 12-11 also illustrates that a larger number of electrons is produced by the more energetic 0.6 Å radiation than the longer-wavelength 5 Å X-rays. Thus, the size of the pulse (the pulse height) is greater for high-frequency X-rays than for low-frequency X-rays.

The Geiger Tube

The Geiger tube is a gas-filled transducer operated in the voltage region between V_5 and V_6 in Figure 12-11; in this region,

gas amplification is greater than 10^9. Each photon produces an avalanche of electrons and cations; the resulting currents are thus large and relatively easy to detect and measure.

The conduction of electricity through a chamber operated in the Geiger region, as well as in the proportional region, is not continuous because the space charge mentioned earlier terminates the flow of electrons to the anode. The net effect is a momentary pulse of current followed by an interval during which the tube does not conduct. Before conduction can again occur, this space charge must be dissipated by migration of the cations to the walls of the chamber. During the *dead time*, when the tube is nonconducting, response to radiation is impossible; the dead time thus represents a lower limit in the response time of the tube. Typically, the dead time of a Geiger tube is in the range from 50 to 200 μs.

Geiger tubes are usually filled with argon; a low concentration of an organic *quenching gas*, often alcohol or methane, is also present to minimize the production of secondary electrons when the cations strike the chamber wall. The lifetime of a tube is limited to some 10^8 to 10^9 counts, when the quencher becomes depleted.

With a Geiger tube, radiation intensity is determined by counting the pulses of current. The device is applicable to all types of nuclear and X-radiation. However, it lacks the large counting range of other detectors because of its relatively long dead time; this factor limits its use in X-ray spectrometers. Although quantitative applications of Geiger tube transducers have decreased, transducers of this type are still frequently used in portable instruments.

Proportional Counters

The proportional counter is a gas-filled transducer that is operated in the V_3 to V_4 voltage region in Figure 12-11. In this region, the pulse produced by a photon is amplified by a factor of 500 to 10,000, but the number of positive ions produced is small enough so that the dead time is only about 1 μs. In general, the pulses from a proportional counter tube must be amplified before being counted.

The number of electrons per pulse, which is proportional to the *pulse height*, produced in the proportional region depends directly on the energy, and thus the *frequency*, of the incoming radiation. A proportional counter can be made sensitive to a restricted range of X-ray frequencies with a *pulse-height analyzer*, which counts a pulse only if its amplitude falls within selectable limits. A pulse-height analyzer in effect permits electronic sorting of radiation; its function is analogous to that of a monochromator.

Proportional counters have been widely used as detectors in X-ray spectrometers.

Ionization Chambers

Ionization chambers are operated in the voltage range from V_1 to V_2 in Figure 12-11. In this region, the currents are small (10^{-13}

to 10^{-16} Å typically) and relatively independent of applied voltage. Ionization chambers are not useful for X-ray spectrometry because of their lack of sensitivity. They are, however, applied in radiochemical measurements, which are discussed in Chapter 32.

Scintillation Counters

The luminescence produced when radiation strikes a phosphor is one of the oldest methods of detecting radioactivity and X-rays, and it is still used widely for certain types of measurements. In its earliest application, the technique involved the manual counting of flashes that resulted when individual photons or radiochemical particles struck a zinc sulfide screen. The tedium of counting individual flashes by eye led Geiger to develop gas-filled transducers, which were not only more convenient and reliable but more responsive to radiation. The advent of the photomultiplier tube (Section 7E-2) and better phosphors, however, has given new life to the technique, and scintillation counting has again become one of the important methods for radiation detection.

The most widely used modern *scintillation detector* consists of a transparent crystal of sodium iodide that has been activated by the introduction of 0.2% thallium iodide. Often, the crystal is shaped as a cylinder that is 3 to 4 in. in each dimension; one of the plane surfaces then faces the cathode of a photomultiplier tube. As the incoming radiation passes through the crystal, its energy is first lost to the *scintillator* and subsequently released in the form of photons of fluorescence radiation. Several thousand photons with a wavelength of about 400 nm are produced by each primary particle or photon over a period of about 0.25 μs, which is the dead time. The dead time of a scintillation counter is thus significantly smaller than the dead time of a gas-filled detector.

The flashes of light produced in the scintillator crystal are transmitted to the photocathode of a photomultiplier tube and are in turn converted to electrical pulses that can be amplified and counted. An important characteristic of scintillators is that the number of photons produced in each flash is proportional to the energy of the incoming radiation. Thus, incorporation of a pulse-height analyzer to monitor the output of a scintillation counter forms the basis of energy-dispersive photometers, which are discussed later.

In addition to sodium iodide crystals, a number of organic scintillators such as stilbene, anthracene, and terphenyl have been used. In crystalline form, these compounds have decay times of 0.01 and 0.1 μs. Organic liquid scintillators have also been developed and are used to advantage because they exhibit less self-absorption of radiation than do solids. An example of a liquid scintillator is a solution of *p*-terphenyl in toluene.

Semiconductor Transducers

Semiconductor transducers have assumed major importance as detectors of X-radiation. The most important of these devices are the *lithium-drifted silicon detector*, Si(Li); the *lithium-drifted germanium detector*, Ge(Li); the *silicon pin photodiode*; and the *silicon drift detector*, SDD.

Figure 12-12 illustrates one form of a lithium-drifted detector, which is fashioned from a wafer of crystalline silicon. There are three layers in the crystal: a *p*-type semiconducting layer that faces the X-ray source, a central *intrinsic* zone, and an *n*-type layer. The outer surface of the *p*-type layer is coated with a thin layer of gold for electrical contact; often, it is also covered with a thin beryllium window that is transparent to X-rays. The signal output is taken from an aluminum layer that coats the *n*-type silicon; this output is fed into a preamplifier with a gain of about 10.
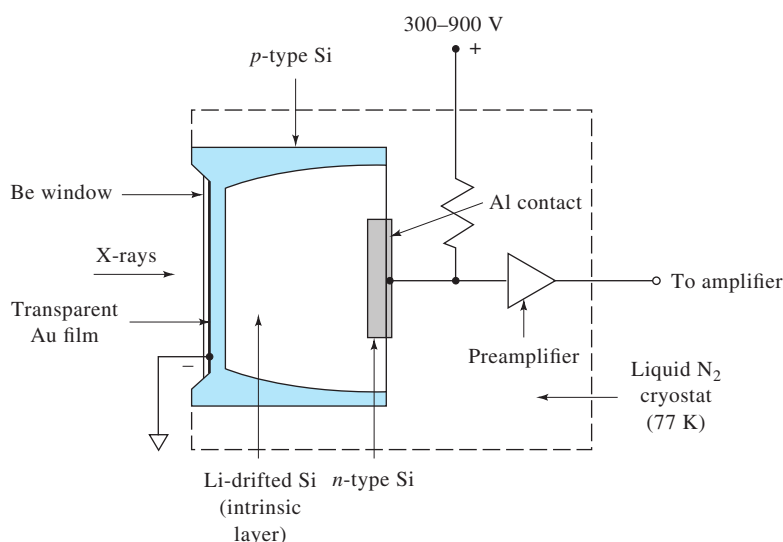
FIGURE 12-12 Vertical cross section of a Si(Li) for X-rays and radiation from radioactive sources.

The preamplifier is frequently a field-effect transistor that is fabricated as an integral part of the detector.

A lithium-drifted detector is formed by vapor-depositing lithium on the surface of a *p*-doped silicon crystal. When the crystal is heated to 400°C to 500°C, the lithium diffuses into the crystal. Because lithium easily loses electrons, its presence converts the *p*-type region to an *n*-type region. While still at an elevated temperature, a dc voltage applied across the crystal causes withdrawal of the electrons from the lithium layer and holes from the *p*-type layer. Current across the *pn* junction causes migration, or drifting, of lithium *ions* into the *p* layer and formation of the intrinsic layer, where the lithium ions replace the holes lost by conduction. When the crystal cools, this central layer has a high resistance relative to the other layers because the lithium ions in this medium are less mobile than the holes they displaced.

The intrinsic layer of a silicon detector functions in a way that is analogous to argon in the gas-filled transducer. Initially, absorption of a photon results in formation of a highly energetic photoelectron, which then loses its kinetic energy by elevating several thousand electrons in the silicon to the conduction band; a marked increase in conductivity results. When a voltage is applied across the crystal, a current pulse accompanies the absorption of each photon. As in proportional detectors, the size of the pulse is directly proportional to the energy of the absorbed photons. Unlike proportional detectors, however, secondary amplification of the pulse does not occur.

As shown in Figure 12-12, the detector and preamplifier of a lithium-drifted detector must be thermostatted at the temperature of liquid nitrogen (77 K) to decrease electronic noise to a tolerable level. The original Si(Li) detectors had to be cooled at all times because at room temperature the lithium atoms would diffuse throughout the silicon, thereby degrading the performance of the detector. Modern Si(Li) detectors need to be cooled only during use.

Germanium is used in place of silicon to give lithium-drifted detectors particularly useful for detection of radiation shorter in wavelength than 0.3 Å. These detectors must be cooled at all times. Germanium detectors that do not require lithium drifting have been produced from very pure germanium. These detectors, called *intrinsic germanium detectors*, need to be cooled only during use.

The *pin* photodiode was previously discussed in Section 7E-2 as a transducer for ultraviolet-visible radiation. This photodiode is also an X-ray transducer. X-ray photons striking the photodiode ionize silicon atoms and produce electron-hole pairs that are swept through the device to produce a current. Each X-ray photon gives rise to a transient current pulse, which can be detected and measured by a charge-sensitive preamplifier connected to the cathode and pulse-processing electronics. The amplitude of the current pulse is directly related to the energy of the incident photon.

The silicon drift detector is very similar to the *pin* photodiode, but uses a very small anode surrounded by ring-shaped drift electrodes. The electrodes form a drift field that is configured so as to guide the electrons through the device to the anode that is usually located in the center of the device. The small area of the anode provides the SDD with much lower capacitance than a normal *pin* photodiode or a Si(Li) detector. This small capacitance leads to lower noise and higher energy resolution than ordinary *pin* diodes, particularly at high counting rates. Silicon drift diodes are more expensive than *pin* photodiodes because of the annular electrodes.

Charge-coupled devices (CCDs) are also used as X-ray detectors. These two-dimensional devices are rapidly replacing traditional imaging detectors (e.g., photographic film) in techniques such as X-ray microscopy, X-ray imaging, micro-XRF imaging, X-ray lithography, and nondestructive X-ray testing. Many X-ray CCD cameras are direct detection devices in which the CCD directly absorbs the incident X-ray photons. Different types of CCD cameras, including back-illuminated and front-illuminated devices, are used depending on the X-ray energy range being explored. Cameras for indirect detection using fiber-optic inputs to the CCD are also available commercially.

Distribution of Pulse-Heights from X-ray Transducers

To understand the properties of energy-dispersive spectrometers, it is important to appreciate that the size of current pulses resulting from absorption of successive X-ray photons of identical energy by the transducer will not be exactly the same. Variations resulting from the ejection of photoelectrons and their subsequent generation of conduction electrons are random processes governed by the laws of probability. Thus, there is a Gaussian distribution of pulse heights around a mean value. The width of this distribution varies from one type of transducer to another, with semiconductor detectors providing significantly narrower bands of pulses. It is this property that has made semiconductor detectors so important for energy-dispersive X-ray spectroscopy.

12B-5 Signal Processors

The signal from the preamplifier of an X-ray spectrometer is the input to a linear fast-response amplifier whose gain can be varied by a factor up to 10,000. Voltage pulses as large as 10 V result.

Pulse-Height Selectors

Most modern X-ray spectrometers (wavelength dispersive as well as energy dispersive) are equipped with *discriminators* that reject pulses of less than about 0.5 V (after amplification). In this way, the contributions of transducer and amplifier noise are reduced significantly. Some instruments have *pulse-height selectors*, or *window discriminators*, which are electronic circuits that reject not only pulses with heights below some predetermined minimum level but also those

above a preset maximum level; that is, they remove all pulses except those that lie within a limited *channel* or *window* of pulse heights.[8]

Dispersive instruments are often equipped with pulse-height selectors to reject noise and to supplement the monochromator in separating the analyte line from higher-order, more energetic radiation that is diffracted at the same crystal setting.

Pulse-Height Analyzers

Pulse-height analyzers consist of one or more pulse-height selectors configured in such a way as to provide energy spectra. A single-channel analyzer typically has a voltage range of about 10 V or more with a window of 0.1 to 0.5 V. The window can be manually or automatically adjusted to scan the entire voltage range, thus providing data for an energy-dispersive spectrum. Multichannel analyzers typically contain up to a few thousand separate channels, each of which acts as a single channel that corresponds to a different voltage window. The signal from each channel is then accumulated in a memory location of the computer or analyzer corresponding to the energy of the channel, thus permitting simultaneous counting and recording of an entire spectrum.

Scalers and Counters

To obtain convenient counting rates, the output from an X-ray transducer is sometimes scaled—that is, the number of pulses is reduced by dividing by some multiple of ten or two, depending on whether the circuit is a decade or a binary device. A brief description of electronic scalers is found in Section 4C-4. Counting of the scaled pulses is carried out with electronic counters such as those described in Sections 4C-2 and 4C-3.

12C X-RAY FLUORESCENCE METHODS

Excitation in an XRF spectrometer is usually accomplished by irradiating the sample with a beam of X-rays from an X-ray tube or a radioactive source. In XRF, elements in the sample are excited by absorption of the primary X-ray beam. They subsequently emit (fluoresce) characteristic X-rays. XRF is a powerful tool for rapid, quantitative determinations of all but the lightest elements in bulk materials, in coatings and in micro-samples. In addition, XRF is used for the qualitative identification of elements having atomic numbers greater that of oxygen (>8) and is often used for semiquantitative or

> **Exercise:** Learn more about **X-ray transducers** at www.tinyurl.com/skoogpia7

quantitative elemental analyses.[9] A particular advantage of XRF is that it is nondestructive, in contrast to most other elemental analysis techniques.

XRF can be used in single- and multiple-point mode, in area examination mode, in linescan mode, and in imaging (mapping) mode. Micro-XRF methods are available for small area examination particularly for irregularly shaped samples.

12C-1 Instruments

Various combinations of the instrument components discussed in the previous section lead to two primary types of spectrometers: *wavelength-dispersive X-ray fluorescence* (WDXRF) and *energy-dispersive X-ray fluorescence* (EDXRF) instruments.[10]

Wavelength-Dispersive Instruments

Wavelength-dispersive instruments always contain tube sources because of the large energy losses that occur when an X-ray beam is collimated and dispersed into its component wavelengths. Radioactive sources produce X-ray photons at a rate less than 10^{-4} that of an X-ray tube; the added attenuation by a monochromator would produce a beam that was difficult or impossible to detect and measure accurately.

Wavelength-dispersive instruments are of two types, *single channel* (or *sequential*) and *multichannel* (or *simultaneous*). The spectrometer shown in Figure 12-9 is a sequential instrument that can be easily used for XRF analysis. In this type of instrument, the X-ray tube and sample are arranged as shown in the circular insert at the top of the figure. Single-channel instruments may be manual or automatic. Manual instruments are quite satisfactory for the quantitative determination of a few elements. In this application, the crystal and transducer are set at the proper angles (θ and 2θ) and counting progresses until sufficient counts have accumulated for precise results. Automatic instruments are much more convenient for qualitative analysis, where an entire spectrum must be scanned. In such a device, the motions of the crystal and detector are synchronized and the detector output is connected to the data-acquisition system.

Most modern single-channel spectrometers are provided with two X-ray sources; typically, one has a chromium target for long wavelengths and the other a tungsten target for short wavelengths. For $\lambda > 2$ Å, it is necessary to remove air between

---

[8]For a discussion of signal shaping, see Section 4C-1.

[9]See M. Haschke, *Laboratory Micro-X-Ray Fluorescence Spectroscopy*, Heidelberg: Springer, 2014; R. Jenkins, *X-Ray Fluorescence Spectrometry*, 2nd ed., New York: Wiley, 1999.

[10]For reviews of X-ray spectrometry including XRF, see K. Tsuji, K. Nakano, Y. Takahashi, K. Hayashi, C.U. Ro, *Anal. Chem.*, **2012**, *84*, 636, **DOI**: 10.1021/ac202871b; *Anal. Chem.*, **2010**, *82*, 4950, **DOI**: 10.1021/ac101069d; P. J. Potts, A. T. Ellis, P. Kregsamer, C. Streli, C. Vanhoof, M. West, and P. Wobrauschek, *J. Anal. Atomic Spectrometry*, **2005**, *20*, 1124, **DOI**: 10.1039/b511542f.
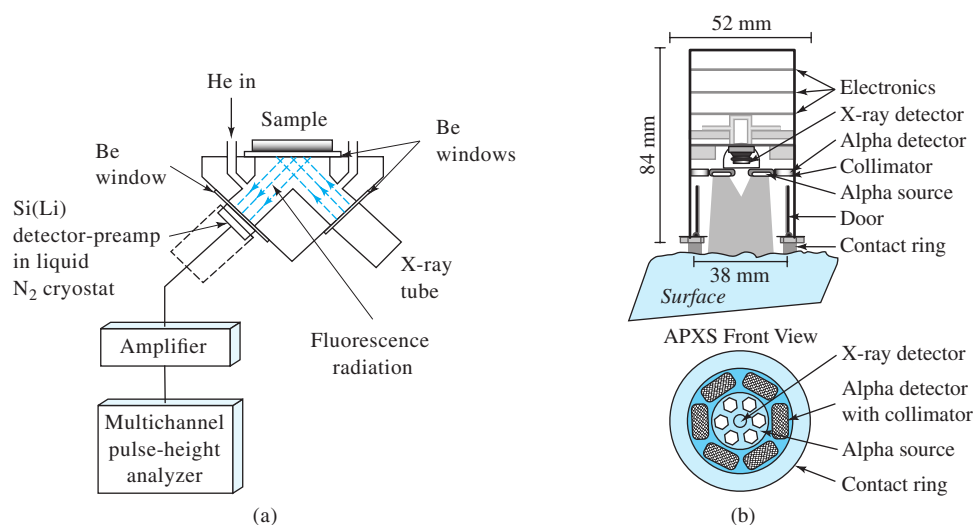
FIGURE 12-13 EDXRF spectrometer. Excitation by X-rays from (a) an X-ray tube and (b) a radioactive substance (curium-244, a 5.81 MeV alpha particle and X-ray source) as shown in the sensor head for the Mars alpha proton X-ray spectrometer. The X-ray detector is a new room-temperature type. (Reprinted with permission from R. Gellert et al., J. Geophys. Res., **2006**, *111*, E02S05, **DOI:** 10.1029/2005je002555.)

the source and detector by pumping or by displacement with a continuous flow of helium. In this type of instrument, dispersing crystals must also be easily interchangeable. Single-channel instruments cost more than $50,000.

Multichannel dispersive instruments are large, expensive (>$150,000) installations that permit the simultaneous detection and determination of as many as twenty-four elements. In these instruments, individual channels consisting of an appropriate crystal and a detector are arranged radially around an X-ray source and sample holder. The crystals for all or most of the channels are usually fixed at an appropriate angle for a given analyte line; in some instruments, one or more of the crystals can be moved to permit a spectral scan.

Each transducer in a multichannel instrument has its own amplifier, pulse-height selector, scaler, and counter or integrator. These instruments are equipped with a computer for instrument control, data processing, and display of analytical results. A determination of twenty or more elements can be completed in a few seconds to a few minutes.

Multichannel instruments are widely used for the determination of several components in industrial materials such as steel, other alloys, cement, ores, and petroleum products. Both multichannel and single-channel instruments are equipped to handle samples in the form of metals, powdered solids, evaporated films, pure liquids, or solutions. When necessary, the materials are placed in a cell with a Mylar or cellophane window.

Energy-Dispersive Instruments

As shown in Figure 12-13a, an EDXRF spectrometer consists of a polychromatic source—which may be either an X-ray tube or a radioactive material—a sample holder, a semiconductor

detector, and the various electronic components required for energy discrimination.[11]

An obvious advantage of energy-dispersive systems is the simplicity and lack of moving parts in the excitation and detection components of the spectrometer. Furthermore, the absence of collimators and a crystal diffractor, as well as the closeness of the detector to the sample, result in a 100-fold or more increase in energy reaching the detector. These features permit the use of weaker sources such as radioactive materials or low-power X-ray tubes, which are cheaper and less likely to cause radiation damage to the sample. Generally, energy-dispersive instruments cost about one fourth to one fifth the price of wavelength-dispersive systems.

Figure 12-13b shows the sensor head from the Mars rover missions of 2004. A similar instrument is aboard the Mars Science Laboratory on the Mars rover Curiosity, which arrived at Gale Crater in 2012. The head contains a curium-244 source that emits X-rays and 5.81 MeV alpha particles. The X-rays cause fluorescence in Martian rock samples, and the alpha particles stimulate X-ray emission as well. X-ray emission stimulated by bombardment by alpha and other subatomic particles such as protons is called *particle induced X-ray emission*, or PIXE. The X-ray detector is a new room-temperature type, which in the low temperature of the Martian night (below −40°C) exhibits low noise and high signal-to-noise ratio for excellent resolution and sensitivity. Note the concentric design of the sensor head with six Cm-244 sources

---

[11]See R. Jenkins, *X-Ray Fluorescence Spectrometry*, 2nd ed., New York: Wiley, 1999.
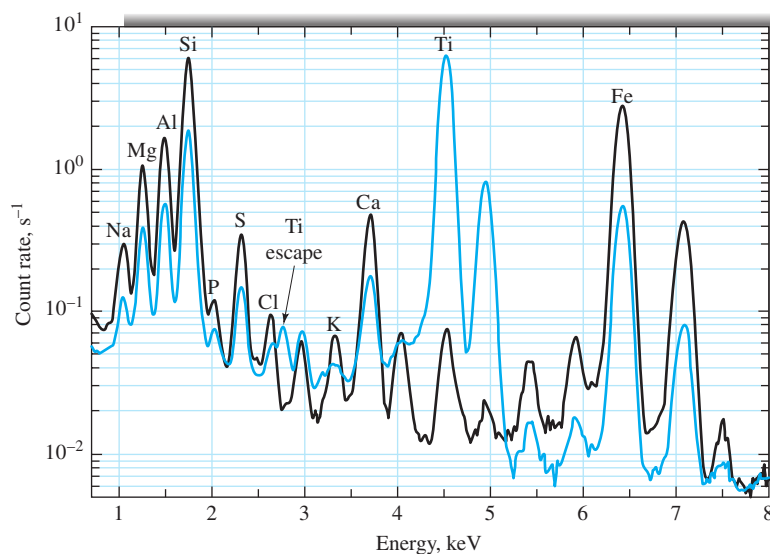
FIGURE 12-14 X-ray spectrum obtained on Mars by the Mars Science Laboratory rover Curiosity on samples taken at Gale Crater. A comparison is shown between in situ particles (Portage, black curve) and those delivered to a Ti observation tray (Sample on o-tray, blue curve). (Reprinted with permission from J. A. Berger et al., *J. Geophys. Res. Planets*, **2014**, *119*, 1046, **DOI**: 10.1002/2013JE004519.

arranged around the central detector. The X-ray spectrum of Figure 12-14 was acquired by the Mars Science Laboratory aboard Curiosity.

In a multichannel, energy-dispersive instrument, all of the emitted X-ray lines are measured simultaneously. Increased sensitivity and improved signal-to-noise ratio result from the Fellgett advantage (see Section 7I-1). The principal disadvantage of energy-dispersive systems, when compared with crystal spectrometers, is their lower resolutions at wavelengths longer than about 1Å . On the other hand, at shorter wavelengths, energy-dispersive systems exhibit superior resolution.

Figure 12-15a is a photo of a basic, commercial, benchtop EDXRF instrument that is used for the routine determination of a broad range of elements from sodium to uranium in samples from many industrial processes. The diagram of Figure 12-15b shows a close-up of the bottom of the sample turntable, which is visible from the top in the photo of Figure 12-15a, and the optical layout of the instrument. Radiation from the X-ray tube passes through an appropriate filter before striking the bottom of the rotating sample. The X-ray fluorescence emitted by the sample passes to the silicon detector, which provides the signal for the multichannel counting system. The system is equipped with a rhodium anode X-ray tube, five programmable filters, a helium purge system, a twelve-position sample changer, and a spinner to rotate each sample during the data-acquisition process. Spinning the sample reduces errors due to sample heterogeneity. We describe a quantitative application of this instrument in Section 12C-3.

Many instrument companies now produce portable (field) and mobile EDXRF spectrometers. These analyzers can be taken to the mining, geological, environmental, or archaeological site rather than transporting samples to the laboratory. Handheld XRF analyzers have become very popular for such testing. Figure 12-15c shows one of these devices. Handheld spectrometers often include X-ray tube sources, but radioactive sources are also used. Detectors are usually SDD-types or *pin* diodes. The unit shown has an X-ray tube with a Rh, Au, or Ta anode and an SDD detector. The unit includes a computer and digital-processing electronics. It is battery operated and weighs a little over 3 lbs without the rechargeable Li-ion battery.

Micro-X-Ray Fluorescence

XRF can be obtained on very small areas by using X-ray optics to focus the incident beam to a small spot size and pinhole apertures to restrict the detected emission. Polycapillary optics and crystal focusing optics have been used to obtain spot sizes of a few micrometers. Confocal geometries with two focusing optics have been used. The drawback to examining such small areas is, of course, diminished intensity of the incident and emitted beams. For this reason, synchrotron sources, with their very high intensities, were first used to obtain micro-X-ray spectra. However, improvements in X-ray optics and in detectors have led to more routine laboratory applications of micro-X-ray methods.[12]

---

[12]See M. Haschke, *Laboratory Micro-X-Ray Fluorescence Spectroscopy*, Heidelberg: Springer, 2014.

(a)

(b)

(c)
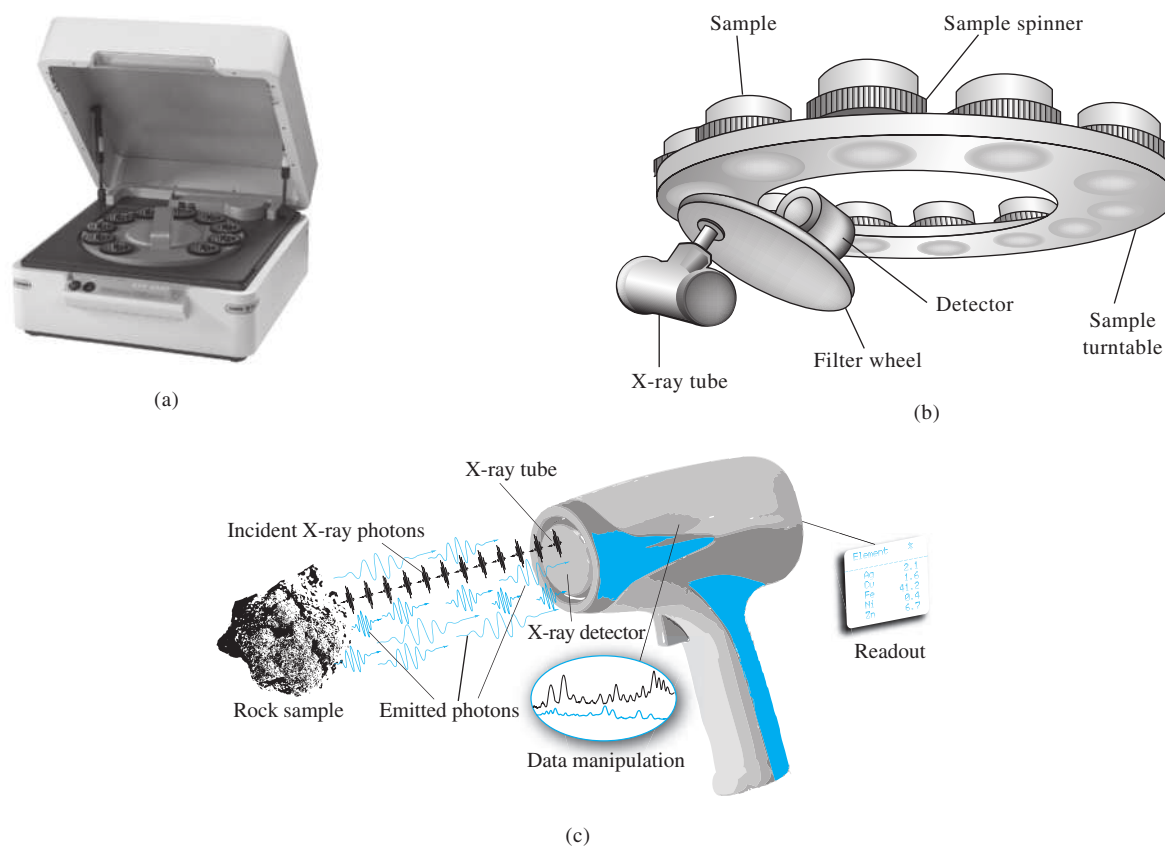
FIGURE 12-15 (a) Epsilon 3^XLE benchtop XRF spectrometer showing removable turntable for up to twelve samples. (b) Diagram showing the X-ray source, filter wheel, detector, and sample turntable from the bottom. (c) Handheld XRF instrument. The radiation from the X-ray tube sources strikes the sample, which emits fluorescent X-rays that are detected by an SDD detector. (Photo in (a) courtesy of PANalytical B.V., Almelo, The Netherlands.)

Since its introduction, micro-XRF has found many applications in the precious metals field, in forensic analysis, in archaeology, and in the analysis of coating layers. Micro-XRF techniques have also been applied to the scanning and imaging of very small samples, such as biological, geological, and semiconductor samples. Although micro-XRF is a relatively new technique, improvements in optics, detection, and sample positioning are already leading to new and unique applications. As an example, the new Mars rover planned for launch in 2020 by NASA will include a micro-XRF instrument designed for fine-scale identification of the composition of rocks and soils on Mars.

Total Reflection X-ray Fluorescence

Total reflection XRF (TRXRF) is a surface technique that has been used to examine particulates, residues, and impurities on smooth surfaces.[13] When the incident beam strikes the sample at angles less than the critical angle for external total reflection,

TRXRF occurs. Usually a thin layer of sample on a smooth substrate is used. Due to the total reflection of the incident beam, only a small portion of this radiation penetrates into the sample substrate which greatly reduces scattering contributions to background and matrix effects. Because the incident beam is totally reflected, the sample is excited by both the incident and the reflected beam, resulting in a near doubling of the fluorescence signal. The grazing incidence also allows for placing the detector very close to the substrate giving a very large solid angle of detection.

Surface contaminations in samples like silicon wafers can be mapped by moving the wafer below the detector. Applications have been made to biological materials, minerals, forensic samples, archaeological samples, paintings, soils, plants, and foods.

12C-2 Qualitative and Semiquantitative Analysis

Figure 12-16 is a spectrum obtained with an energy-dispersive instrument. With such equipment, the abscissa is generally calibrated in channel number or energy in keV. Each dot represents the number of counts accumulated in one of the several hundred channels.

---

[13]R. Klockenkamper and A. von Bohlen, *Total Reflection X-Ray Fluorescence Analysis and Related Methods*, 2nd ed., Hoboken, NJ: Wiley, 2015.
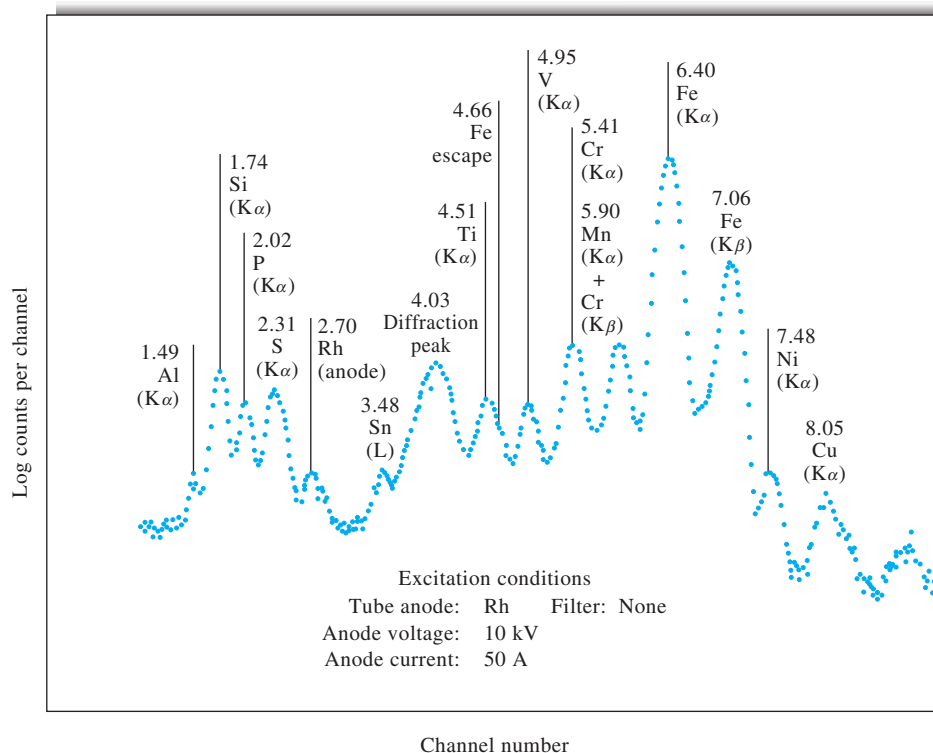
FIGURE 12-16 Spectrum of an iron sample obtained with an energy-dispersive instrument with a Rh anode X-ray tube source. The numbers above the peaks are energies in keV. (Reprinted with permission from J. A. Cooper, *Amer. Lab.*, **1976**, *8* (11), 44. Copyright 1976 by International Scientific Communications, Inc.)

Qualitative information, such as that shown in Figures 12-16, can be converted to semiquantitative data by careful measurement of peak heights. To obtain a rough estimate of concentration, the following relationship is used:

$$P_x = P_s W_x \qquad (12\text{-}7)$$

where P_x is the relative line intensity measured in terms of number of counts for a fixed period, and W_x is the weight fraction of the desired element in the sample. The factor P_s is the relative intensity of the line that would be observed under identical counting conditions if W_x were unity. The value of P_s is determined with a sample of the pure element or a standard sample of known composition.

The use of Equation 12-7, as outlined in the previous paragraph, carries with it the assumption that the emission from the species of interest is unaffected by the presence of other elements in the sample. This assumption is often not justified. As a result, concentration estimates may be in error by a factor of 2 or more. On the other hand, this uncertainty is significantly smaller than that associated with a semiquantitative analysis by optical emission where order-of-magnitude errors are not uncommon.

12C-3 Quantitative Analysis

Modern XRF instruments are capable of producing quantitative analyses of complex materials with precision greater than or equal to that of the classical wet chemical methods or other instrumental methods.[14] For the accuracy of such analyses to approach this level, however, requires either the availability of calibration standards that closely approach the samples in overall chemical and physical composition or suitable methods for dealing with matrix effects.

Matrix Effects

It is important to realize that the X-rays produced in the fluorescence process are generated not only from atoms at the surface of a sample but also from atoms well below the surface. Thus, a part of both the incident radiation and the resulting fluorescence traverse a significant thickness of sample within which absorption and scattering can occur. The extent either beam is attenuated

[14]See R. E. Van Grieken and A. A. Markowicz, eds., *Handbook of X-Ray Spectrometry*, 2nd ed., New York: Marcel Dekker, 2002; R. Jenkins, R. W. Gould, and D. Gedcke, *Quantitative X-Ray Spectrometry*, 2nd ed., New York: Marcel Dekker, 1995.

depends on the mass absorption coefficient of the medium, which in turn is determined by the absorption coefficients of *all* of the elements in the sample. Therefore, although the net intensity of a line reaching the detector in an XRF measurement depends on the concentration of the element producing the line, the concentration and mass absorption coefficients of the matrix elements affect it as well. An exception to this is TRXRF where grazing incidence leads to little penetration into the sample or substrate.

Absorption effects by the matrix may cause results calculated by Equation 12-7 to be either high or low. If, for example, the matrix contains a significant amount of an element that absorbs either the incident or the emitted beam more strongly than the element being determined, then W_x will be low, because P_s was evaluated with a standard in which absorption was smaller. On the other hand, if the matrix elements of the sample absorb less than those in the standard, high values for W_x result.

A second matrix effect, called the *enhancement effect*, can also yield results that are greater than expected. This behavior occurs when the sample contains an element whose characteristic emission spectrum is excited by the incident beam, and this spectrum in turn causes a secondary excitation of the analytical line.

Several techniques have been developed to compensate for absorption and enhancement effects in XRF analyses.

External Standard Calibration

The relationship between the analytical line intensity and the concentration must be determined empirically with a set of standards that closely approximate the samples in overall composition. We then assume that absorption and enhancement effects are identical for samples and standards, and the empirical data are used to convert emission data to concentrations. The degree of compensation achieved in this way depends on the closeness of the match between samples and standards.

Use of Internal Standards

In this procedure, an element is introduced in known and fixed concentration into both the calibration standards and the samples; the added element must be absent in the original sample. The ratio of the intensities between the element being determined and the internal standard is the analytical variable. The assumption here is that absorption and enhancement effects are the same for the two lines and that use of intensity ratios compensates for these effects.

Dilution of Samples and Standards

Both sample and standards are diluted with a substance that absorbs X-rays only weakly, that is, a substance containing elements with low atomic numbers. Examples of such diluents include water; organic solvents only containing carbon, hydrogen, oxygen, and nitrogen; starch; lithium carbonate; alumina; and boric acid or borate glass. By adding a diluent in excess, matrix effects become essentially constant for the

diluted standards and samples, and adequate compensation is achieved. This procedure has proved particularly useful for mineral analyses, where both samples and standards are dissolved in molten borax; after cooling, the fused mass is excited in the usual way.

Methods and Data Analysis for Multiple Elements

When it is possible to establish that total sample X-ray absorption does not vary appreciably over an expected range of analyte concentrations and when enhancement effects are absent, we generally find a linear relationship between XRF line intensity and element concentration.[15] When such conditions occur, it is often possible to use *type standardization* techniques. In these techniques, standards are prepared and characterized or, more often, purchased from the National Institute of Standards and Technology (NIST) or other sources. These standards are then used to calibrate spectrometers and establish the working curves for analysis. Hundreds of such standards are available for matching samples with particular types of standards.

When the nature and composition of the sample is not well known, it is necessary to use *influence correction methods*, of which there are three primary types: *fundamental*, *derived*, and *regression*. In the fundamental approach, the intensity of fluorescence can be calculated for each element in a standard sample from variables such as the source spectrum, the fundamental equations for absorption and fluorescence, matrix effects, the crystal reflectivity (in a WDXRF instrument), instrument aperture, the detector efficiency, and so forth. The XRF spectrum of the standard is measured, and in an iterative process the instrument variables are refined and combined with the fundamental variables to obtain a *calibration function* for the analysis. Then the spectrum for an unknown sample is measured, and the iterative process is repeated using initial estimates of the concentrations of the analytes. Iteration continues until the calculated spectrum matches the unknown spectrum according to appropriate statistical criteria. This method gives good results with accuracies on the order of 1–4% but is generally considered to be less accurate than derived or regression methods.[16] So-called *standardless analysis* is accomplished using variations on fundamental calibration methods. Instruments are carefully characterized, and instrument and fundamental parameters are stored in the computer. Spectra are then calculated and matched with samples by iterative methods to estimate concentrations of analytes.

Derived methods simplify calculations of the fundamental method by lumping detailed fundamental calculations into generalized parameters to account for instrument functions, but the calculation of fluorescence intensities from analyte

[15]R. Jenkins, *X-Ray Fluorescence Spectrometry*, 2nd ed., New York: Wiley, 1999, pp. 182–186.

[16]J. L. de Vries and B. A. R. Vrebos, in R. E. Van Grieken and A. A. Markowicz, eds., *Handbook of X-Ray Spectrometry*, 2nd ed., New York: Marcel Dekker, 2002, p. 378.

concentration is the same as in fundamental methods. Derived methods often show some improvement in accuracy and precision over fundamental methods.

Regression methods rely on models of the form

$$W_i = B_i + K_i I_i \left[1 + \sum_{j=1}^{n} m_{ij} W_{ij} \right]$$

where B_i is the background, K_i is a sensitivity coefficient, I_i is the intensity due to element i, m_{ij} is the *binary influence coefficient* that describes the matrix effect of element j on analyte i, and W_{ij} is the average composition of the sample in i and j. To calibrate an instrument, spectra are acquired for standards and regression analysis is performed to determine K_i, B_i, and m_{ij} for each binary combination of elements in the standards. These parameters are then used in a regression analysis of spectral data from unknown samples to determine the unknown concentrations W_i. A broad range of models and algorithms for regression analysis in XRF are available, and many commercial instruments use combinations and variations on these algorithms in their software suites.[17] Accuracies and precisions attained using these methods are typically 1% or better under optimal conditions. Regression methods were used to analyze the data of Figure 12-14 from the Mars rover to determine by EDXRF the concentrations of many elements in rocks and soil.

In the early days of XRF, influence correction methods were difficult and time-consuming because sufficient computational power to accomplish them was available only on large, expensive mainframe computers. With the advent of powerful, low-cost, dedicated computers, sophisticated data analysis is now routine, and all commercial instruments have mature software suites for instrument operation, calibration, data reduction, and analysis.

Some Quantitative Applications of X-ray Fluorescence

With proper correction for matrix effects, XRF spectrometry is one of the most powerful tools available for the rapid quantitative determination of all but the lightest elements in complex samples. For example, Rose, Bornhorst, and Sivonen[18] have demonstrated that twenty-two elements can be determined in powdered rock samples with a commercial EDXRF spectrometer in about 2 hours (1 hour instrument time), including grinding and pellet preparation. Relative standard deviations for the method are better than 1% for major elements and better than 5% for trace elements. Accuracy and detection limits as determined by comparison to results from international standard rock samples were comparable or better than other published

procedures. For an excellent overview of XRF analysis of geological materials, see the paper by Anzelmo and Lindsay.[19]

X-ray methods are also applied widely for quality control in the manufacture of metals and alloys. Because of the speed of the analysis in these applications, it is possible to correct the composition of the alloy during its manufacture.

XRF methods are easily adapted to liquid samples. Methods have been devised for the direct quantitative determination of lead and bromine in aviation fuel samples. Similarly, calcium, barium, and zinc have been determined in lubricating oils by exciting fluorescence in the liquid hydrocarbon samples. Conventional XRF, micro-XRF, and TRXRF are also convenient for the direct determination of pigments in paint samples.

XRF methods are being widely applied to the analysis of atmospheric pollutants. For example, one procedure for detecting and determining contaminants involves drawing an air sample through a stack consisting of a micropore filter for particulates and three filter paper disks impregnated with orthotolidine, silver nitrate, and sodium hydroxide, respectively. The reagents retain chlorine, sulfides, and sulfur dioxide in that order. The filters containing trapped analytes then serve as samples for XRF analysis.

As an example of the routine application of EDXRF for determining the elemental composition of foodstuffs, consider the plots of Figure 12-17a and 12-17b.[20] In this analysis, iron, copper, and zinc were determined in rice using a spectrometer similar to that shown in Figure 12-15a. The spectrometer was calibrated using nine standard samples of rice. The standards were ground into fine powders, pressed into pellets, and loaded into the sample turntable. Each sample was irradiated with X-rays (Rh anode) through an aluminum filter for 5 minutes, and data were acquired to produce spectra such as the one shown in Figure 12-17a. The instrument computer then analyzed the data and calculated the areas under the various peaks in the spectrum as shown by the shaded areas in the figure, and calibration curves similar to Figure 12-17b were produced for each of the analytes. Determination of the analytes in another well-characterized sample yielded concentrations of 73.49 ppm, 7.46 ppm, and 38.95 ppm for iron, copper, and zinc, respectively. Relative accuracies for the three elements were 0.9% (Fe), 5% (Cu), and 0.3% (Zn) as determined by comparison with values determined by optical spectroscopic methods.

Another indication of the versatility of XRF is its use for measuring the elemental composition of particulates and rock samples in the Gale Crater on Mars. The spectrum shown in Figure 12-14 was obtained by the Mars Science Laboratory aboard the rover Curiosity. Such measurements combined with

[17]Ibid., pp. 341–405.

[18]W. I. Rose, T. J. Bornhorst, and S. J. Sivonen, *X-Ray Spectrometry*, **1986**, *15*, 55, **DOI**: 10.1002/xrs.1300150111.

[19]J. E. Anzelmo and J. R. Lindsay, *J. Chem. Educ.*, **1987**, *64*, A181. **DOI**: 10.1021/ed064pA181 and A200, **DOI**: 10.1021/ed064pA200.

[20]V. Sethi, M. Mizuhira, and Y. Xiao, *G.I.T. Laboratory Journal*, **2005**, *6*, 22.
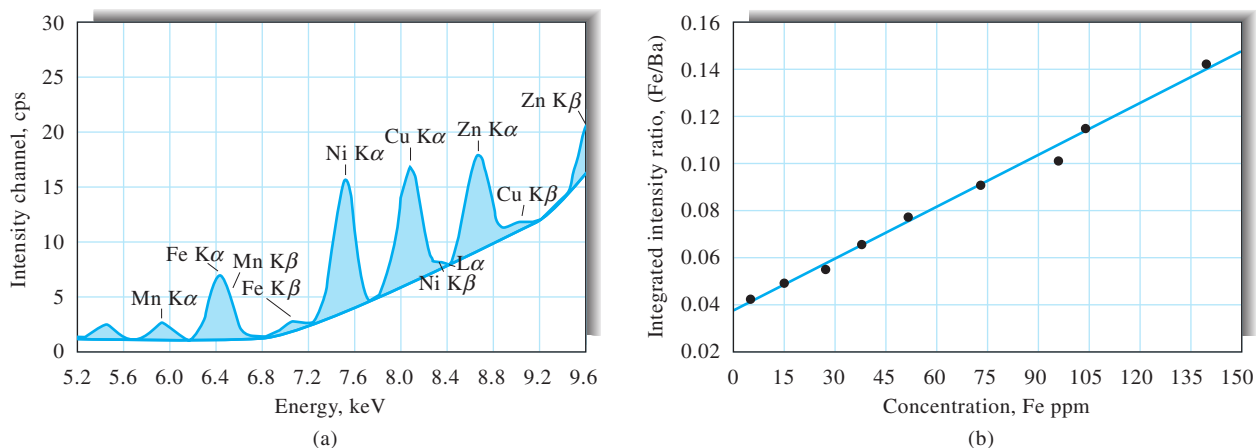
FIGURE 12-17 (a) XRF spectrum of rice sample. The shaded areas under the curve are proportional to the amount of each element in the sample. (b) Calibration curve obtained from nine rice samples. Integrated areas from spectra similar to that in (a) are plotted against certified concentrations of iron. (Reprinted with permission from V. Sethi, M. Mizuhira, and Y. Xiao, *G.I.T. Laboratory Journal*, **2005**, *6*, 22. Copyright by GIT Verlag Gmbh & Co.)

others allow the chemical composition of Martian samples to be obtained.[21] The Mars 2020 mission will include a micro-XRF instrument mounted on the robotic arm of the rover.

Combination of XRF with Other Methods

XRF can be effectively combined with other methods. One of the most useful combinations is that of a scanning electron microscope (SEM) with an EDXRF spectrometer (see Section 21F-2). In this method, the sample is scanned by the electron beam of the SEM, which can excite fluorescence from the sample. With this combination, it is possible to obtain an SEM image along with elemental information at any point on the image. Micro-XRF can be combined with an SEM by adding an X-ray tube and focusing optics to an existing SEM instrument.

XRF has also been combined with Raman and infrared spectroscopy. With these techniques, structural information and organic composition can be added to the elemental information provided by XRF. XRF combined with X-ray diffraction makes it possible to use elemental composition information with the phase analysis of X-ray diffraction. Knowledge of chemical composition can make phase analysis faster and more accurate.

Advantages and Disadvantages of X-ray Fluorescence Methods

XRF offers a number of impressive advantages. The spectra are relatively simple, so spectral line interference is minimal. Generally, the X-ray method is nondestructive and can be used for the analysis of paintings, archaeological specimens, jewelry, coins, and other valuable objects without harm to the sample. Furthermore, analyses can be performed on samples ranging

from micrometer diameters to relatively massive objects. Other advantages include the speed and convenience of the procedure, which permit multielement analyses to be completed in a few minutes. Finally, the accuracy and precision of XRF methods often equal or exceed those of other methods.[22]

XRF methods are generally not as sensitive as the optical methods discussed earlier. Except for TRXRF, where trace amounts can be detected, the concentration range of most XRF methods is from about 0.01% to 100%. XRF methods for the lighter elements are inconvenient; difficulties in detection and measurement become progressively worse as atomic numbers become smaller than 23 (vanadium), in part because a competing process, called *Auger emission* (see Section 21C-2), reduces the fluorescence intensity (see Figure 21-7). Today's commercial instruments have a lower atomic number limit of 5 (boron) or 6 (carbon).

12D X-RAY ABSORPTION METHODS

X-ray absorption spectroscopy (XAS), sometimes called X-ray absorption fine structure spectroscopy (XAFS), can provide chemical and physical information about a target element. The information can include oxidation state, coordination number, and local structure. The technique has element selectivity and is

Tutorial: Learn more about **applications of X-ray fluorescence** at www.tinyurl.com/skoogpia7

---

[21]See, for example, D. F. Blake et al., *Science*, **2013**, *341*, 1239505, **DOI**: 10.1126/science.1239505.

[22]For a comparison of XRF and inductively coupled plasma for the analysis of environmental samples, see T. H. Nguyen, J. Boman, and M. Leermakers, *X-Ray Spectrometry*, **1998**, *27*, 265, **DOI**: 10.1002/(SICI)1097-4539 (199807/08)27:4<265::AID-XRS296>3.0.CO;2-3

applicable to samples in many different forms (crystalline, amorphous, solution, colloidal, etc.). X-ray absorption has been used in a two-dimensional mapping mode and a three-dimensional imaging mode. In contrast to optical spectroscopy where quantitative absorption methods are most important, analytical XAS applications are somewhat limited when compared to XRF methods. Because matrix effects can be a major problem in quantitative applications, most analyses are confined to samples in which matrix effects are minimal.

Quantitative XAS methods are analogous to optical absorption procedures in which the attenuation of a band or line of X-radiation is the analytical variable. Wavelength selection is accomplished with a monochromator such as that shown in Figure 12-9 or by a filter technique similar to that illustrated in Figure 12-8. Alternatively, the monochromatic radiation from a radioactive source may be used.

Because of the width of X-ray absorption peaks, direct absorption methods are generally useful only when a single element with a high atomic number is to be determined in a matrix consisting of only lighter elements. Examples of applications of this type are the determination of lead in gasoline and the determination of sulfur or the halogens in hydrocarbons.

12D-1 X-ray Diffraction Methods

Since its discovery in 1912 by von Laue, X-ray diffraction has provided a wealth of important information to science and industry. For example, much of what is known about the arrangement and the spacing of atoms in crystalline materials has been determined directly from diffraction studies. In addition, such studies have led to a much clearer understanding of the physical properties of metals, polymeric materials, and other solids. X-ray diffraction is one of the most important methods for determining the structures of such complex natural products as steroids, vitamins, and antibiotics. The details of these applications are beyond the scope of this book.

X-ray diffraction also provides a convenient and practical means for the qualitative identification of crystalline compounds. The X-ray powder diffraction method is the only analytical method that is capable of providing qualitative and quantitative information about the *compounds* present in a solid sample. For example, the powder method can determine the percentage KBr and NaCl in a solid mixture of these two compounds. Other analytical methods reveal only the percentage K^+, Na^+, Br^-, and Cl^- in the sample.[23]

Because each crystalline substance has a unique X-ray diffraction pattern, X-ray powder methods are well suited for qualitative identification. Thus, if an exact match can be found

between the pattern of an unknown and an authentic sample, identification is assured.

12D-2 Identification of Crystalline Compounds

Sample Preparation

For analytical diffraction studies, the crystalline sample is ground to a fine homogeneous powder. In such a form, the enormous number of small crystallites are oriented in every possible direction; thus, when an X-ray beam passes through the material, a significant number of the particles are oriented in such ways as to fulfill the Bragg condition for reflection from every possible interplanar spacing.

Samples are usually placed in a sample holder that uses a depression or cavity to mount the sample. These mounts are commonly made of aluminum, bronze, Bakelite, glass, or Lucite. Cavity mounts are most commonly side loaded or back loaded. A frosted glass surface, ceramic, or cardboard is placed over the front, and the sample is carefully added via the open side or back. Top-loading mounts are also available as are special mounts known as zero background mounts. Alternatively, a specimen may be mixed with a suitable noncrystalline binder and molded into an appropriate shape.

Automatic Diffractometers

Diffraction patterns are generally obtained with automated instruments similar in design to that shown in Figure 12-9. In this instrument, the source is an X-ray tube with suitable filters. The powdered sample, however, replaces the single crystal on its mount. In some instances, the sample holder may be rotated to increase the randomness of the orientation of the crystals. The diffraction pattern is then recorded by automatic scanning in the same way as for an emission or absorption spectrum. Instruments of this type offer the advantage of high precision for intensity measurements and automated data reduction and report generation.

Diffraction Patterns

The classical photographic method for recording powder diffraction patterns is still used, although the use of X-ray CCD cameras is increasing. The most common instrument for this purpose is the *Debye-Scherrer* powder camera, which is shown schematically in Figure 12-18a. Here, the beam from an X-ray tube is filtered to produce a nearly monochromatic beam (often the copper or molybdenum Kα line), which is collimated by passage through a narrow tube.

Figure 12-8 shows how a filter can be used to produce a relatively monochromatic beam. Note that the Kβ line and most of the continuum from a Mo target are removed by a zirconium filter with a thickness of about 0.01 cm. The pure Kα line is then available for diffractometry. Several other target-filter

---

[23]For a more detailed discussion of the X-ray powder diffraction method, see R. Jenkins and R. Snyder, *Introduction to X-Ray Powder Diffractometry*, New York: Wiley, 1996.
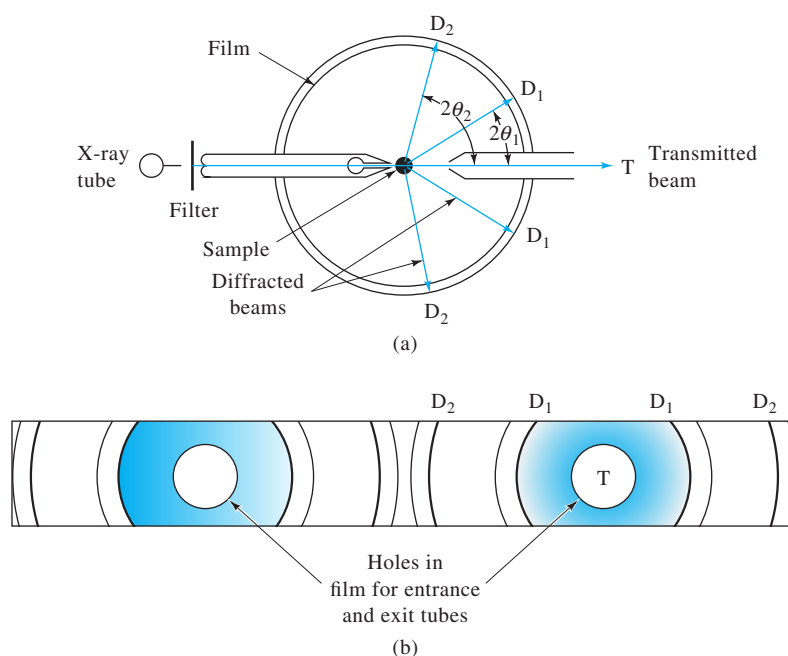
FIGURE 12-18 Schematic of (a) a Debye-Scherrer powder camera; (b) the film strip after development. D_2, D_1, and T indicate positions of the film in the camera.

combinations have been developed to isolate one of the intense lines of the target material.

The undiffracted radiation T then passes out of the camera via a narrow exit tube as shown in Figure 12-18a. The camera itself is cylindrical and equipped to hold a strip of film around its inside wall. The inside diameter of the cylinder usually is 5.73 or 11.46 cm, so that each lineal millimeter of film is equivalent to 1.0° or 0.5° in θ, respectively. The sample is held in the center of the beam by an adjustable mount.

Figure 12-18b shows the appearance of the exposed and developed film; each set of lines (D_1, D_2, and so forth) represents diffraction from one set of crystal planes. The Bragg angle θ for each line is easily evaluated from the geometry of the camera.

12D-3 Interpretation of Diffraction Patterns

The identification of a species from its powder diffraction pattern is based on the position of the lines (in terms of θ or 2θ) and their relative intensities. The diffraction angle 2θ is determined by the spacing between a particular set of planes; with the aid of the Bragg equation, this distance d is calculated from the known wavelength of the source and the measured angle. Line intensities depend on the number and kind of atomic reflection centers in each set of planes.

Crystals are identified empirically. A powder diffraction database is maintained by the International Centre for Diffraction Data, Newtown Square, Pennsylvania. As of 2013, the database contained powder diffraction patterns for more

than 800,000 materials. Because the file is so large, the powder data file has been broken down into subfiles that contain listings for inorganics, organics, minerals, metals, alloys, forensic materials, and others. The sub-databases are available via the Internet and a USB dongle with an access key, and software is available for searching the databases using any combination of several search criteria. Each record in the database contains a wealth of information regarding the substances and materials, including name, formula (if appropriate), composition, color, line strengths, melting point, mineral classification, density, and a host of other characteristics of the materials as well as bibliographic information. A variety of presentation modes are available so that graphs and other important images may be viewed and printed.[24]

If the sample contains two or more crystalline compounds, identification becomes more complex. Here, various combinations of the more intense lines are used until a match can be found. Computer searching and matching of data greatly facilitates this task.

One very important application is the determination of the percentage crystallinity of materials. In the analysis of polymeric and fibrous materials, determining the crystalline-to-amorphous ratio has long been of importance, and X-ray powder methods have unique advantages in these determinations. In the pharmaceutical area, the degree of crystallinity can influence the long-term stability of a formulation as well as its

---

[24]For further information regarding the powder diffraction database, see http://www.icdd.com/.

bioactivity. X-ray diffraction methods are being increasingly applied to pharmaceuticals.

Crystalline materials produce well-defined diffraction peaks whose widths are related to the crystalline "quality." High-quality materials produce sharp peaks, and poor-quality materials give rise to more diffuse diffraction peaks. Amorphous phases come in different forms depending on how they were formed. A glassy phase produces a diffraction signal that is the radial distribution of nearest neighbor interactions. An amorphous phase derived from a crystalline phase usually corresponds to a poor-quality, or paracrystalline, material. Both glassy and paracrystalline specimens produce a low-frequency halo, which can appear as a broad background.

One approach to determining the crystalline-to-amorphous ratio is to use conventional quantitative analysis methods. Non-overlapped X-ray diffraction peaks are chosen for the phase to be analyzed. Either peak height or peak area is used for quantitative analysis. Standards of known concentration are then used to prepare a calibration curve.

In the Vainshtein approach, the amorphous phase is used as a normalizing factor for the integrated intensities of the crystalline peaks.[25] This eliminates the effects of sample preparation and instrument drift. Analysis is based on *Vainshtein's law*, which states that the diffracted intensity from a material is independent of its state of order within identical regions of reciprocal space. To apply the law, a single standard with a

known percentage of crystallinity is used to establish the normalization ratio between the integrated crystalline peaks and the amorphous "background." The same measurements are then made on the specimen of unknown crystallinity. The percentage crystallinity of the unknown is then found from

$$\%C_u = \%C_{std}\left[\frac{(C/A)_u}{(C/A)_{std}}\right] \qquad (12\text{-}8)$$

where $\%C_u$ and $\%C_{std}$ are the percentage crystallinities of the unknown and standard respectively, and C/A is the ratio of the integrated intensity of the crystalline phase C to the amorphous background A.

Yet another approach is to use Fourier transform methods to split the power spectrum into low- and high-frequency regions. The amorphous phase is associated with the low-frequency region, and the crystalline phase is associated with the high-frequency region. After filtering the undesired region, the inverse transform gives the amorphous intensity and the crystalline intensity. Standards are used to determine the width and frequencies of the filters.

12E THE ELECTRON MICROPROBE

An important method for the determination of the elemental composition of surfaces is based on the *electron microprobe*. In this technique, X-ray emission from the elements on the surface of a sample is stimulated by a narrowly focused beam of electrons. The resulting X-ray emission is detected and analyzed with either a wavelength or an energy-dispersive spectrometer. This method is discussed further in Section 21F-1.

---

[25]B. K. Vainshtein (1921–1996) was a prominent Russian X-ray crystallographer. His monograph *Diffraction of X-rays by Chain Molecules* (Amsterdam: Elsevier, 1966) played an important role in the development of structural studies of polymers.

»» QUESTIONS AND PROBLEMS

*Answers are provided at the end of the book for problems marked with an asterisk.

X▦ Problems with this icon are best solved using spreadsheets.

*12-1 What is the short-wavelength limit of the continuum produced by an X-ray tube having a tungsten target and operated at 50 kV?

*12-2 What minimum tube voltage would be required to excite the $K\beta$ and $L\beta$ series of lines for (a) U, (b) K, (c) Cr, and (d) Cs?

12-3 The $K\alpha_1$ lines for Ca, Zn, Zr, and Sn have wavelengths of 3.36, 1.44, 0.79, and 0.49 Å, respectively. Calculate an approximate wavelength for the $K\alpha$ lines of (a) V, (b) Ni, (c) Se, (d) Br, (e) Cd, and (f) Sb.

12-4 The $L\alpha$ lines for Ca, Zn, Zr, and Sn have wavelengths of 36.3, 11.9, 6.07, and 3.60 Å, respectively. Estimate the wavelengths for the $L\alpha$ lines for the elements listed in Problem 12-3.

*12-5 The mass absorption coefficient for Ni, measured with the Cu $K\alpha$ line, is 49.2 cm^2/g. Calculate the thickness of a nickel foil that was found to transmit 35.2% of the incident power of a beam of Cu $K\alpha$ radiation. The density of Ni is 8.90 g/cm^3.

» QUESTIONS AND PROBLEMS (continued)

* **12-6** For Mo Kα radiation (0.711 Å) the mass absorption coefficients for K, I, H, and O are 16.7, 39.2, 0.0, and 1.50 cm^2/g, respectively.

(a) Calculate the mass absorption coefficient for a solution prepared by mixing 11.00 g of KI with 89.00 g of water.

(b) The density of the solution described in (a) is 1.086 g/cm^3. What fraction of the radiation from a Mo Kα source would be transmitted by a 0.40-cm layer of the solution?

* **12-7** Aluminum is to be used as windows for a cell for X-ray absorption measurements with the Ag Kα line. The mass absorption coefficient for aluminum at this wavelength is 2.74; its density is 2.70 g/cm^3. What maximum thickness of aluminum foil could be used to fabricate the windows if no more than 2.8% of the radiation is to be absorbed by them?

* **12-8** A solution of I$_2$ in ethanol had a density of 0.794 g/cm^3. A 1.50-cm layer was found to transmit 33.2% of the radiation from a Mo Kα source. Mass absorption coefficients for I, C, H, and O are 39.2, 0.70, 0.00, and 1.50, respectively.

(a) Calculate the percentage of I$_2$ present, neglecting absorption by the alcohol.

(b) Correct the results in part (a) for the presence of alcohol.

* **12-9** Calculate the goniometer setting, in terms of 2θ, required to observe the Kα_1 lines for Fe (1.76 Å), Se (0.992 Å), and Ag (0.497 Å) and Ag (0.497 Å) when the diffracting crystal is (a) topaz, (b) LiF, and (c) NaCl.

12-10 Calculate the goniometer setting, in terms of 2θ, required to observe the Lβ_1 lines for Br at 8.126 Å when the diffracting crystal is

(a) ethylenediamine d-tartrate.

(b) ammonium dihydrogen phosphate.

* **12-11** Calculate the minimum tube voltage required to excite the following lines. The numbers in parentheses are the wavelengths in Å for the corresponding absorption edges.

(a) K lines for Ca (3.064)

(b) Lα lines for As (9.370)

(c) Lβ lines for U (0.592)

(d) K lines for Mg (0.496)

12-12 Manganese was determined in samples of geological interest via XRF using barium as an internal standard. The fluorescence intensity of isolated lines for each element gave the following data:

Wt. % Mn	Ba	Mn
0.00	156	80
0.10	160	106
0.20	159	129
0.30	160	154
0.40	151	167

What is the weight percentage manganese in a sample that had a Mn-to-Ba count ratio of 0.936?

Challenge Problem

12-13 As discussed in Section 12C-3, the APXS, or alpha proton X-ray spectrometer, has been an important experiment aboard all of the Mars exploration rovers. Journal articles provide details of the APXS experiments on the missions in 2004 and compare the instrumentation and measurement strategies with those on board the Pathfinder mission of 1997.[26]

(a) Consult the cited articles, and describe the construction and operation of the detector head on the Mars rovers. Illustrate your answer with basic diagrams of the instrument components, and describe the function of each.

(b) What determines the selectivity and sensitivity of the APXS system?

(c) What elements cannot be determined by APXS? Why not?

(d) Characterize the general elemental composition of all of the Martian landing sites. What are the similarities and differences among the sites. What explanation do these workers and others give for the similarities?

(e) How were the APXS measurements limited by the time in the Martian day when the experiments were completed? Explain the cause of these limitations. How and why were the APXS experiments terminated?

(f) What effect did temperature have on the results of the X-ray mode of the APXS experiments? How does this effect relate to your discussion in (e)?

(g) The APXS experiments were used to compare the surface composition with the composition of the interiors. How was this accomplished? What differences were discovered? What explanation was given for the differences?

(h) Halogen fractionation was apparent in the Martian rock samples. What explanation was given for this phenomenon?

(i) Characterize the overall precision and accuracy of the APXS experiments. The APXS team states that "accuracy is mainly determined by precision." Explain what is meant by this statement. Under what circumstances is it true?

(j) Explain in some detail the calibration procedure for the APXS experiments. What calibration standards were used on Mars, and where were they located? How were individual element peaks extracted from the X-ray spectra?

(k) Figure 12-19 shows a plot of corrected calibration data for Fe from the APXS experiments. Note that there are uncertainties in both the x and y data. The data from the plot are tabulated in the following table. Carry out a normal least-squares analysis of the data using Excel. Determine the slope, intercept, correlation coefficient, and the standard deviation about regression.

[26]R. Gellert et al., *J. Geophys. Res.*, **2006**, *111*, E02S05, **DOI**: 10.1029/2005je002555; S. W. Squyres et al., *J. Geophys. Res.*, **2003**, *108*, 8062, **DOI**: 10.1029/2003je002121; R. Rieder et al., *J. Geophys. Res.*, **2003**, *108*, 8066, **DOI**: 10.1029/2003je002150; J. Brückner et al., *J. Geophys. Res.*, **2003**, *108*, 8094, **DOI**: 10.1029/2003je002060; R. Gellert et al., *Science*, **2004**, *305*, 829, **DOI**: 10.1126/science.1099913; H. Y. McSween et al., *Science*, **2004**, *305*, 842, **DOI**: 10.1126/science.3050842; S. W. Squyres et al., *Science*, **2004**, *306*, 1709, **DOI**: 10.1126/science.1104559; L. A. Soderblom et al., *Science*, **2004**, *306*, 1723, **DOI**: 10.1126/science.1105127; G. Klingelhofer et al., *Science*, **2004**, *306*, 1740, **DOI**: 10.1126/science.1104653; R. Rieder et al., *Science*, **2004**, *306*, 1746, **DOI**: 10.1126/science.1104358; A. Banin, *Science*, **2005**, *309*, 888, **DOI**: 10.1126/science.1112794.

» QUESTIONS AND PROBLEMS (continued)

Peak Area	σ	Mass %	σ
2.36	0.28	2.12	0.13
7.04	0.54	5.75	0.13
6.68	0.54	5.85	0.13
8.01	0.39	7.14	0.10
8.42	0.44	7.45	0.13
9.04	0.44	7.87	0.10
14.74	0.74	13.20	0.10
17.93	0.90	15.58	0.18
21.27	1.05	20.24	0.21
23.22	1.18	20.71	0.23
25.02	1.26	20.55	0.18

(l) Carry out a weighted least-squares analysis of the data using a procedure similar to the one described in Problem 10-14 that allows for uncertainties in both the x and y variables. Compare your results to those obtained in (k).
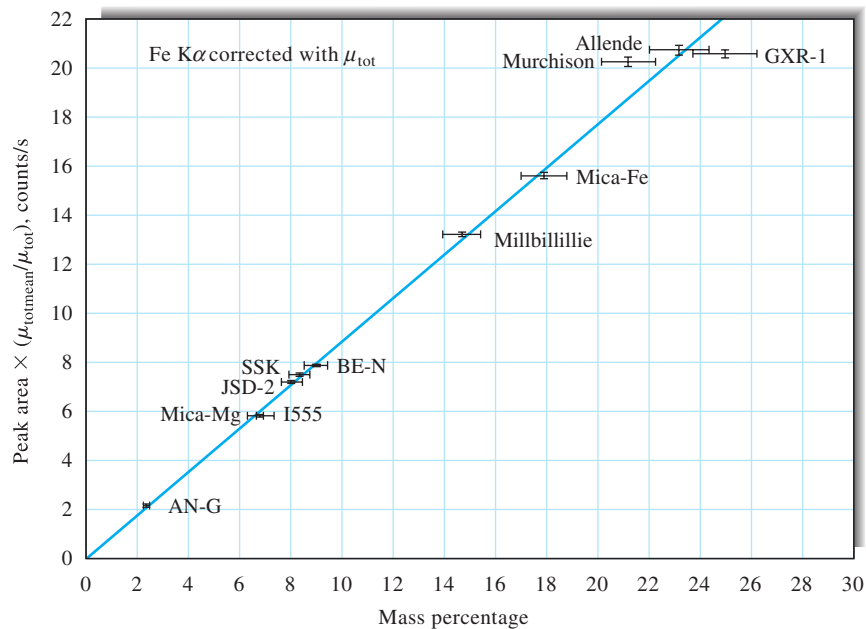
FIGURE 12-19 APXS calibration curve for Fe corrected for attenuation coefficient. (From R. Rieder et al., *J. Geophys. Res.,* **2003,** *108,* 8066, **DOI:** 10.1029/2003je002150, with permission.)

Monitoring Mercury

Mercury is an extremely important element in the environment, in foods, and in industrial processes. The health scares concerning mercury have been many since the best-known case, the Minamata Bay disaster in Japan in 1956. Minamata is a small industrial town on the coast of the Shiranui Sea. The major industrial firm in Minamata, the Chisso Corporation, dumped some 37 tons of mercury-containing compounds into Minamata Bay from 1932 to 1968. As a result, thousands of local residents, whose normal diet included fish from the bay, developed symptoms of methylmercury poisoning. The disease became known as *Minamata disease*. Since then, there have been many warnings about eating fish and shellfish known to contain high levels of mercury. The most recent recommendations of the United States Environmental Protection Agency (EPA) and the Food and Drug Administration warn women of child-bearing age and young children not to eat shark, swordfish, king mackerel, or tilefish. These agencies also advise women and young children to eat no more than 12 ounces per week of fish that contain lower levels of mercury, such as shrimp, canned tuna, salmon, pollock, tilapia, cod, and catfish. More stringent recommendations apply to fish from certain lakes, rivers, and coastal areas.

Sources of Mercury

Mercury is, of course, a naturally occurring element. However, industrial pollution is a major source of environmental mercury. The pollution comes from many sources, such as coal-burning power plants, refineries, runoff from factories, and industrial waste. Mercury also enters the environment from such sources as automobile exhausts, sewage treatment plants, medical and dental facilities, and water runoff from mercury- and gold-mining operations. The Clean Air Act, first enacted in the United States in 1963 with major amendments in 1970, 1977, and 1990, mandated levels of air pollution, including mercury. Likewise, the EPA has set water-quality criteria for levels of mercury in both fresh and saltwater systems.[1] The Clean Water Act requires that individual states achieve safe concentration levels for pollutants like mercury.

Mercury from the air or from water sources accumulates in streams and lakes. Bacteria in the water convert the mercury into methylmercury, which is readily absorbed by insects and other aquatic organisms. The mercury-containing compounds rapidly move up the food chain as small fish eat the small organisms and big fish eat the small fish. The concentrations of mercury are determined by the life span of the fish and its feeding habits. The highest concentrations are found in large fish such as swordfish and sharks.

Instrumental Analysis in Action

determined by the life span of the fish and its feeding habits. The highest concentrations are found in large fish such as swordfish and sharks.

Analytical Chemistry Challenges

Because of its importance in the environment, accurate, reliable determinations of mercury are crucial. Although determination of the various forms that mercury takes in the environment is of interest, current regulations focus on measurements of total mercury, which is in itself challenging. The challenge arises because in complex environmental samples mercury is present in very small amounts. The EPA has established a level of 2 ppb for drinking water, 12 ppt (parts per trillion) as the upper limit for freshwater ecosystems, and 25 ppt as the limit for saltwater. The National Toxics rule of the EPA[2] recommends that the safe level for mercury is as low as 1.3 ppt. Frequently, concentrations lower than this criterion are found for total dissolved mercury (inorganic plus organic forms) in seawater. Some ocean surface waters have been found to have concentrations lower than 0.05 ppt, and intermediate water layers can have levels as high as 2 ppt. These low concentrations can be near or lower than the limits of detection for many analytical techniques. In freshwater systems, much higher concentrations have been observed. In some California lakes, for example, levels of 0.5 to 100 ppt have been determined. In any case, detection of these ultratrace levels can be quite a challenge for analytical chemists.

Traditional Methods for Determining Mercury

The concentrations of interest in satisfying regulations in the United States and the United Kingdom are in the parts-per-trillion range and lower. However, conventional analytical methods such as flame atomic absorption, inductively coupled plasma atomic emission, and inductively coupled plasma mass spectrometry cannot achieve parts-per-trillion detection limits because the use of nebulizers to transfer samples to the atomizer is quite inefficient (often only 2% or less of the sample is transferred).[3]

Cold-vapor atomic absorption (see Section 9A-3) can achieve detection limits of a few parts per trillion. In the most sensitive EPA cold-vapor atomic absorption method, the sample is digested with a permanganate-persulfate solution, which oxidizes all the mercury forms to Hg(II). Stannous chloride ($SnCl_2$) is then used to reduce the Hg(II) to elemental mercury, which is swept into the observation cell of the atomic absorption
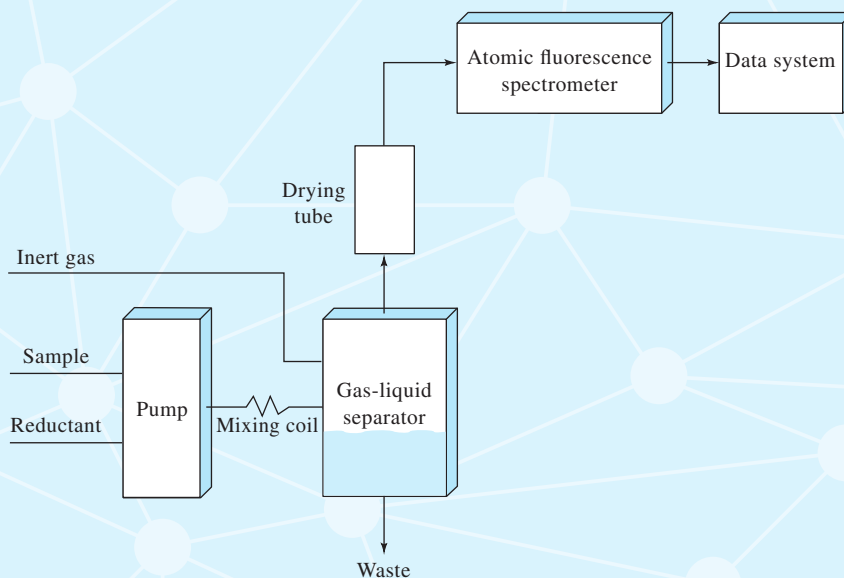
[1]*Quality Criteria for Water*, EPA 440/5-86-001, US Environmental Protection Agency, Office of Water Regulation and Standards, 1986.

[2]http://www.epa.gov/mercury/report.htm.

[3]"Monitoring the Mercury Menace," P. Stockwell, *Today's Chemist at Work*, p. 27, November 2003; http://tinyurl.com/hnbhqj2.

Instrumental Analysis in Action (continued)

FIGURE IA2-1 Cold-vapor atomic fluorescence system for ultratrace determinations of mercury.

spectrometer by a stream of inert gas. Method 245.1 of the EPA[4] can achieve parts per trillion sensitivity with a dynamic range of 2–3 orders of magnitude. EPA method 7474 uses a microwave digestion procedure and has a range from about 1 ppb to several parts per million.

Atomic Fluorescence Methods

Because regulatory requirements are becoming more stringent, it is desirable to have a more sensitive method for mercury. Atomic fluorescence spectrometry (AFS; see Section 9E) can achieve the required detection limits when combined with newly developed cold-vapor technology. Several instrument companies now market mercury analyzers based on AFS. Concurrent with development of commercial atomic fluorescence spectrometers for mercury monitoring has been the development of vapor generation techniques based on liquid-gas-separation technology. With these systems, essentially 100% of the sample is introduced into the spectrometer observation cell. Scattering of light from water vapor is also eliminated.

A block diagram of a cold-vapor atomic fluorescence instrument for mercury determination is given in Figure IA2-1. Here, the predigested and oxidized sample is mixed with $SnCl_2$ or another suitable reductant to generate elemental mercury. A gas-liquid separator is then used to separate the liquid reagents from the mercury vapor, which is transferred to the observation

cell by a stream of inert gas. A high-intensity mercury vapor lamp excites atomic fluorescence.

The EPA method 245.7 uses a system similar to Figure IA2-1 for mercury detection.[5] In some commercial systems, the digestion-oxidation step is also automated. The digestion is with a mixture of HCl, Br^-, and BrO_3^-. The method can achieve a detection limit of 0.1 to 0.2 ppt.

EPA method 1631[6] uses oxidation followed by a purge-and-trap method and cold-vapor atomic fluorescence. Mercury is preconcentrated in the gold-coated sand trap by amalgamation. One commercial instrument uses an atomic fluorescence detection system and claims a working range from <0.05 ppt to ~250 ppb. This method is quite useful for a variety of sample types ranging from seawater to sewage.

Conclusions

Measurements of mercury at the ultratrace levels demanded by current regulations are feasible with cold-vapor AFS. However, great care must be taken to assure high reliability. Getting rid of mercury when high levels are found in the environment is, however, another problem.

[4]*Determination of Mercury in Water by Cold Vapor Atomic Absorption Spectrometry*. EPA Method 245.1, US Environmental Protection Agency, Office of Water, Rev. 3.0, 1994, http://tinyurl.com/jsm768p.

[5]*Mercury in Water by Cold Vapor Atomic Fluorescence Spectrometry*, EPA-821-R-05-001, US Environmental Protection Agency, Office of Water, 2005; http://tinyurl.com/zu753d7.

[6]*Mercury in Water by Oxidation, Purge and Trap, and Cold Vapor Atomic Fluorescence Spectrometry*, Method 1631, Revision E, EPA-821-R-02-019, US Environmental Protection Agency Office of Water, 2002; http://tinyurl.com/jomwyqn.